Journal of Mining and Environment (JME), Vol. 15, No. 2, 2024, 731-759

Shahrood University of Technology

Journal of Mining and Environment (JME)

Journal homepage: www.jme.shahroodut.ac.ir

Iranian Society of Mining Engineering (IRSME)

Soil Arching and Ground Deformation around Tunnels in Sandy Grounds: Review and New Insights

Ghorban Khandouzi[1], and Mohammad Hossein Khosravi[2]*

1. School of Mining Engineering, College of Engineering, University of Tehran, Tehran, Iran
2. Department of Mining Engineering, Faculty of Engineering, University of Birjand, Birjand, Iran

Article Info

Received 30 September 2023
Received in Revised form 31 October 2023
Accepted 14 November 2023
Published online 14 November 2023

DOI: 10.22044/jme.2023.13676.2532

Keywords

Tunnel convergence
Soil arching
Stress redistribution
Non-linear shear bands
Loosened zone

Abstract

Granular materials used in engineering structures tend to experience arching under different geotechnical factors. Arching is a factor of load transfer from the destroyed zone to stable areas in these structures. Soil arching plays an important role in stress redistribution, settlement, and load on supports in tunneling. This paper reviews the effect of various parameters on the development of soil arching and formation of expansion and contraction zones around the tunnel. A comprehensive literature review, analysis of new published papers, and investigations were conducted to study the effects of various parameters on soil arching. The results were obtained by studying the formation of shear bands, deformed zones, and their development. The achieved results of investigations show that soil arching and ground deformation around tunnels in sandy grounds are complex phenomena that require careful consideration during tunnel construction. Also, the results reveal that despite the arching zone, a loosened zone with non-linear slip surfaces forms above the tunnel. With the onset of tunnel convergence, initial non-linear sliding surfaces appear, and the arching area forms above the tunnel. When tunnel convergence increases, a stable arch forms inside the arching zone, and a de-stressed area as a loosened zone is created under the stable arch. Understanding of soil arching, ground deformation, and the stable arch formed inside the arching zone around tunnels in sandy grounds is very important for the engineers evaluating stress redistribution and load on tunnel supports. Also understanding these issues can help the designers and practitioners make informed decisions during tunnel construction.

1. Introduction

Due to the increasing urbanization around the world, tunneling has become a preferred method for transportation and underground systems. Tunnels with concrete supports are one of the types used in urban environments. Designing these tunnels to satisfy environmental conditions and ensure sustainability requires the use of new types of concrete in their construction. New types of concrete has more advantages than conventional ones due to the use of industrial waste that enhances the resistance properties of concrete and reduces environmental pollution. The use of coal ash, marble waste powder, waste molecular sieves instead of sand as water-absorbing fine aggregates, and basalt fiber in concrete are examples of industrial waste [1]. Golewski (2023) investigated the combined effect of siliceous fly ash (FA), silica fume (SF), and nano-silica (nS), and also the effect of coal fly ash (CFA) and nano-silica (nS) on the morphology of cement matrix and size of microcracks occurring in the interfacial transition zone (ITZ) between the coarse aggregate and the cement, the strength, and microstructure properties of concrete. The combined use of 5% nS and 15% CFA can enhance the mechanical parameters of concrete by filling the pores and microcracks in concrete composites. Also when concretes based on quaternary blended cements containing 80% Ordinary Portland Cement (OPC) + 10% SF + 5% FA + 5% nS were used, the width of microcracks reduced, and a more compact and homogeneous structure of the cement matrix in the QBC concrete

Corresponding author: mh.khosravi@birjand.ac.ir (M. Khosravi)

was achieved [2-4]. In addition, in choosing a suitable concrete for the type of construction, the design of the structure should also be considered. Golewski (2022) investigated the importance of limit state calculations in the base of footing, monolithic pocket foundation (PF) wall design, choosing the appropriate type of construction technology in terms of reinforcement preparation, the correct shaping of the foundation, and checking the accuracy of project implementation [5]. Also with the increasing number of tunnels being constructed, it is crucial to have a comprehensive understanding of the displacements and induced stresses caused by tunneling and their impact on adjacent structures [6-11]. Many numerical and experimental researches have been conducted to investigate the stress field, in some of which the non-linearity of stress distribution has been related to the effect of soil arching [12-17].

Stress redistribution resulting from relative displacement or tunnel convergence is a known behavior experienced in both granular and cohesive soils. The permanence of stress redistribution resulting from relative displacement is not similar for granular and cohesive soils. In cohesive soils, the creep phenomenon causes stress to relax over time and often returns to values near those due to the overburden weight. A similar relaxation process can happen in granular soils when subjected to external influences such as vibration. Under this condition, typical reductions observed within granular soils change from insignificant values to only about 15 percent of the stress redistribution caused by soil arching [18].

Soil arching resulting from stress redistribution widely exists in nature such as Karst area and civil engineering including retaining walls, foundations, and tunnels, and is known as a universal phenomenon in the field and laboratory scale. At macroscopic scale, soil arching is a transfer of load from mobilized parts of the soil to stationary portions, and is widely considered in geotechnical projects [19-22].

This phenomenon was first discovered by French military engineers during silo construction. In 1895, Janssen developed an analytical relation for determining the load distribution in silos, based on simplified assumptions. In 1958, Jakobson modified the Janssen's equation based on a non-uniform stress distribution assumption [23, 24]. Marston developed an equation in 1930 using Janssen's silo theory and arching effect to evaluate the load acting on buried conduits. Marston's study between 1920 and 1930 led to the significance of the arching effect for tunnels and other engineering structures [18, 23]. In 1936, Terzaghi experimentally studied the arching effect around tunnels using some trapdoor tests. In 1943, he adopted the concept of soil arching to formulate his analytical approach based on simplified assumptions including vertical slip surface, plain strain condition, and forces equilibrium [25]. Spangler and Handy adopted Marston's experiences in 1973, and developed a modified formulation [26].

From 1962 to 1975, the structural analogy was extended to explain the arching effect and the load distribution around a yielding structure. This comparison led to the ground arch (Dome) approach. Whitman *et al.* (1963) made observations from small-scale tests on thin metal domes buried within coarse sand based on the mentioned theory. They found that the level of pressure required to cause the failure of the buried dome was several times of that required for the failure of an unburied dome [27]. Luscher and Hoeg (1965) attributed this issue to three types of processes: pressure redistribution, deformation restraint, and arching [28]. Getzler *et al*. (1968) proposed a structural analogy for arching in experiments with structures having various roof shapes. An interesting conclusion from their experiment was that buried structures with arch shape experience greater load reduction than structures with flat roofs [29]. These conclusions had good agreement with Whitman's results in 1963 [27].

Despite the structural analogy from 1962 to 1975, analytical methods were extended to estimate the load on structures when the arching phenomenon occurred. Finn (1960) presented the change in vertical stress resulting from the translation or rotation of a trapdoor using a closed-form solution [30]. Finn's studies were limited to infinite overburden depth and low displacements. Therefore, Chelapati (1964) extended Finn's work to account for material self-weight and finite depth of overburden [31]. Bjerrum *et al*. (1972) believed that Chelapati's elastic solution can be further extended to give approximate values for the change in vertical stress [32]. Burghignoli (1981) took Bjerrum's approach one step further, and extended it to underground openings with flexible roofs [33]. Many researchers performed various meaningful works about stress distribution in a linear elastic medium while developing an analytical solution for estimating the stress field by considering the arching effect. Approaches to this issue can be found in Richard (1964), Rohmaller (1968), Board (1971), and Muir Wood (1975) [18]. Recently, Rui

et al. (2018) derived the load distribution equation for three models of soil arching pattern observed in 2D trapdoor test set up including the triangular expanding pattern, tower shape pattern, and equal settlement pattern. They compared the calculated stress-distribution ratio with the results of Terzaghi (1943) and Carlsson (1987). It was indicated that the proposed method has a reasonable match with mentioned methods [34]. Liang *et al*. (2022) performed an experimental test with a trapdoor setup, and introduced an analytical solution to predict the earth pressure acting on top of the trapdoor in the loosened zone. They considered the deflection of the principal stress axis in their solution, and observed good agreement between the analytical prediction and test results [35]. Khandozi and Khosravi (2023) developed a new two-dimensional analytical method based on the arching effect to estimate the stress field inside the soil mass above a tunnel, as shown in Figure 1 [6].

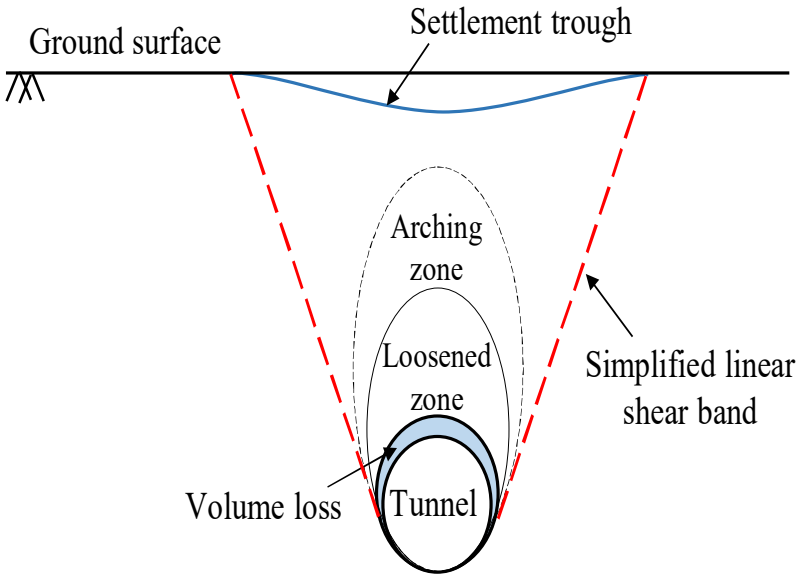

Figure 1. The arching and loosened zones developed above a circular tunnel with assumed linear shear bands [6].

Besides the analytical method and its limitations due to simplified assumptions, in 1970s, the researchers used computer-based techniques to study arching problems. Numerical methods were more flexible than other solutions, leading to the development of numerical solutions for arching issues. Getzler *et al*. (1970) used a finite differential method to analyze the arching of elastic soil [36]. Ranken and Ghaboussi (1975) simulated an advancing tunnel using an axisymmetric finite element program [37]. Rude (1982) predicted the behavior of a culvert using a linear elastic finite element program [38]. Stone (1988) performed non-linear finite element analyses of trap door tests, and correctly predicted an initial soil localization from the edge of the trapdoor into the overlying soil [39]. Koutsabeloulis and Griffiths (1989) simulated a finite element analysis of the trapdoor problem by considering soil as a perfectly plastic material. Based on simulation results, the load on the trap door drops as it is lowered; after the load drops down, instead of increasing again, it stays at a constant value [40]. Sakaguchi and Ozaki (1992) analyzed the formation of arches using the discrete element method. Their analyses were subjected to granular particles during discharging out of a silo due to gravity. They considered rolling friction among particles in their studies [41]. Their numerical results were in good agreement with experimental measures not only in flow pattern but also in the formation of arches. In the recent years, numerical modeling allows for more realistic analyses that consider the tunnel-line interaction, construction sequence, and 3D face effects. Bhandari (2010) studied the soil arching development and the effect of cyclic loading and geosynthetic reinforcement on soil arching by using physical model and the discrete element method [42]. Lin *et al*. 2019 simulated the 3D EPBS tunnel excavation using the finite element method in the PLAXIS software to evaluate the effect of tunnel convergence on the stress distribution, settlement, and the effect of arching in the sand environment. Their modeling results

showed the formation of two zones called loosened and arched zones at the top of the tunnel crown with heights equal to 0.73 and 1.25 tunnel diameters [16]. Geore and Dasaka (2021) modeled the trapdoor mechanism numerically, and studied the suitability of the hardening soil constitutive model over the Mohr-Coulomb model. In their research, they described two families of failure surfaces, internal and external, and classified them with respect to the H/B ratio. They also explained that the dimensions of the influence zone depend on the fill height (H) and trapdoor width (B). Furthermore, they classified the zone of yielding and the region enclosed within limits of influence and failure planes as active and passive zones [43]. Su *et al*. (2022) using finite element software established a refined numerical model for segmental lining of a shield tunnel. The model contains detailed models of reinforcement and connecting bolts. The internal force distribution and the transverse deformation characteristics of the shield tunnel when it is subject to local soil loosening are investigated. The influence of loosening position, loosening range, and loosening extent on the mechanical response is investigated. The results indicated that the main influence of soil loosening on the ring is duo to disturb the force balance, thus changing the deformation pattern. After the loosening happens, the bending moment of the ring increases and the axial force reduces. Also the vertical convergence of the ring increases with increasing loosening extent [44]. Al-Hattamleh *et al*. (2022) used a double-slip gradient model in the ABAQUS finite element software to simulate the effects of arching in dry sand and consider microstructural effects. They performed numerical simulations to model the trap-door setup, and found that strains begin to localize and form shear bands. They also observed that the pattern of plastic strains depends on the orientation of the initial slip system. While arching effects were observed to initiate early with trap-door movement, its maximum effect is observed after full localization. The variation of normalized vertical stress reaches a maximum value around a normalized height of 0.8 above the trap-door irrespective of the orientation of the initial slip system [45].

Despite the numerical model, many researchers have conducted comprehensive studies using software packages such as PFC. Regarding numerical methods, it is necessary to define the appropriate behavioral model and input data despite their flexibility and applicability for different geometries and complex conditions of engineering problems. However, these methods are time-consuming and expensive, especially when the trial-and-error method is used until the input data is aligned in the modeling.

In addition to classical, analytical, and numerical methods for studying the effect of arching on underground structures, empirical approaches have also been developed. Empirical methods generally assume that a loosening zone exists above the underground structure. The loosening zone may have different shapes depending on the assumptions and derivations in this method. Furthermore, the force acting on the structure is assumed to be the weight of the material within the loosening zone plus surcharges. In general, there are two approaches to empirical methods. One approach takes into account the effect of overburden depth (including Bierbaumer (1913), Balla (1963), and Terzaghi (1943)), and the other neglects it [18, 23]. The important point is that empirical methods are quick and simple. If engineers find conditions similar to those presented in the empirical approach, they can accurately predict the behavior of the environment and excavated structure. However, there is uncertainty in the application of empirical methods due to simplifying assumptions used in these methods that may conflict with real conditions.

Empirical, analytical, and numerical research of arching phenomenon has deficiencies and problems. Therefore, many researchers tend to use experimental methods in their research. After Terzaghi's trapdoor test, several researchers including McNulty (1965), Ladanyi and Hoyaux (1969), Harris (1974), and Evans (1984) have duplicated the experiments conducted by Terzaghi (1943) with modifications to the apparatus and testing method [18]. Different physical modeling techniques include the trap door tests (Chen *et al*., 2010; Iglesia *et al*., 2013; Rui *et al*., 2016; Khatami *et al*., 2019; Wu *et al*., 2019; Xu *et al*., 2019; Liang *et al*., 2020) as shown schematically in Figure 2, rigid tube with flexible or movable face (Sterpi *et al*., 1996; Kamata and Masimo, 2003), Pressurized air bags (Atkinson and potts 1977; Wu and Lee 2003; Lee *et al*. 2006), Polystyrene foam and organic solvent (Sharma *et al*., 2001), soil augering (Champan *et al*., 2006), the miniature tunnel boring machines (Nomoto *et al*. 1999) and mechanically adjustable tunnel diameter (Boonsiri and Takemura 2015; Moussaei *et al*. 2019; Moussaei *et al*. 2022; Song and Marshall 2020) used to simulate the process of tunnel excavation and soil displacement [46].

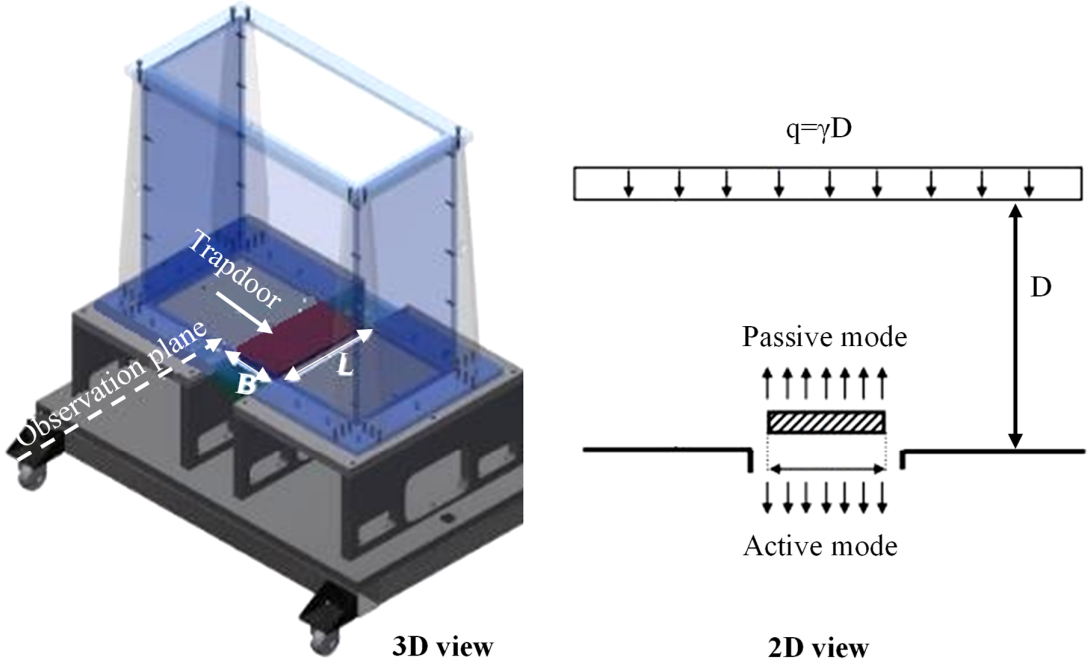

Figure 2. The trapdoor problem [46, 47].

These experimental studies showed when the displacement in soil mass increased, more than stress redistribution, the slip surfaces of the mobilized part were changed too. In the recent years, Costa *et al*. (2009) with experimental results and from previous research including Terzaghi (1936), Evans (1983), Vardoulakis *et al*. (1981), Tanaka and Sakai (1993), and Santichaianaint (2002) explained that the slip surface formation for trapdoors under deep conditions differed obviously from the shallow conditions [48]. Iglesia *et al*. (2011, 2013) performed centrifuge tests to investigate the progress of soil arching with the displacement of the trapdoor and suggested a ground reaction curve (GRC-ground reaction curve is defined as a curve that describes the pressure changes or progressive development of the soil arching ratio with the relative displacement), which is classified into four stages: (1) initial soil arching, (2) maximum soil arching (i.e. the minimum stress on the trapdoor), (3) stress recovery, and (4) ultimate state [49, 50]. Zhang *et al*. (2016) stated that the shearing bands extended from the corners of the trapdoor changed from inward oblique curves to vertical lines as the trapdoor displacement increases from several millimeters to a few centimeters, and then to outward oblique lines [51]. Bhandari and Han (2018) conducted a series of two-dimensional trapdoor tests to investigate soil displacements above double and single trapdoors with or without reinforcement. The researchers used analogical soil made of aluminum bars as embankment and paper as reinforcement. They investigated two different embankment heights and concluded that both reinforcement and embankment height decreased the vertical displacement on the top of the embankment [52]. Rui *et al*. (2019) performed a 2D trapdoor tests without and with geosynthetic reinforcement and found a localized deformation layout (concentric ellipse pattern-CEP or concentric arch-CA) when geosynthetic reinforcement was used [53]. Also Al-Naddaf *et al*. (2019) performed a 2D trapdoor test without and with geosynthetic reinforcement. He presented that the displacement of the trapdoor led to the progressive mobilization of soil arching. He also showed that the geosynthetic reinforcement reduced soil arching mobilization due to the change of the soil deformation. This phenomenon resulted in increasing the applied surface load required to destroy soil arching [54]. Ali *et al*. (2020) investigated the effect of particle shape and size on soil arching and stress field. They found that particle shape has a larger effect on stress than particle size. The authors stated that the angularity of particle shape increases particle interlocking and contact force between them, which leads to the

formation of strong force chain along the arch with the movement of trapdoor [55]. Moussaei *et al*. (2022) performed a series of physical modelling to evaluate the tunnel convergence on soil arching above the tunnel crown. They concluded when the tunnel convergence increased the vertical stress deviated from linear distribution [56]. Zhang *et al*. (2023) conducted a study to investigate the progressive failure of Qanat tunnel. The authors performed three model tests on dry sand to consider the effect of tunnel depth on soil arching and progressive failure. Based on the experimental results, the failure of Qanat tunnel starts from the vault and develops upward, which is related to the evaluation of stress contour. For the deep Qanat tunnel, the collapse of deep tunnel and ground earth pressure can be divided into a stress-increasing region, stress-decreasing region, and no redistribution region [57]. Furthermore, other methods have taken into account the arching effect in the prediction of stress redistribution around underground structures with complicated geometry. One of these techniques is the photo-elasticity method. In this method, stresses are induced and stored in an elastic material like epoxy resin. The material is then sliced and analyzed under polarizing filters. However, the application of this method to arching at present is limited since actual soil cannot be used as the medium for tests and epoxy resin has properties considerably different from granular soil [23].

Due to the lack of comprehensive studies and complete research regarding active arching, passive arching, and stress redistribution in the deformed zone, it is necessary to present complete studies regarding the arching effect in sandy soil. Therefore, this paper presents stress redistribution in the deformed zone and the condition of the formation of active and passive arching in the second section. Then the effect of major parameters on the creation and extension of the slip surface and the behavior mechanism of sandy soil around the tunnel is discussed in the third section. Finally, this paper presents the relationship between the formation of shear bands, the shape and development of the deformed zone, the arching effect, and stress redistribution in sandy soil.

2. Soil Arching

When a portion of a rigid support yields, the adjoining soil moves relative to the remainder of the soil mass. This movement is resisted by shearing stresses that reduce the pressure on the yielding portion of the soil while increasing the pressure on the adjacent stable portions. This phenomenon is known as arching. There are generally two types of arching in soil mass: active arch, where paths of the minor principal stress are continued, and passive arch, where trajectories of the major principal stress are continued [21]. Figure 3 demonstrates the difference between these two types of arching.

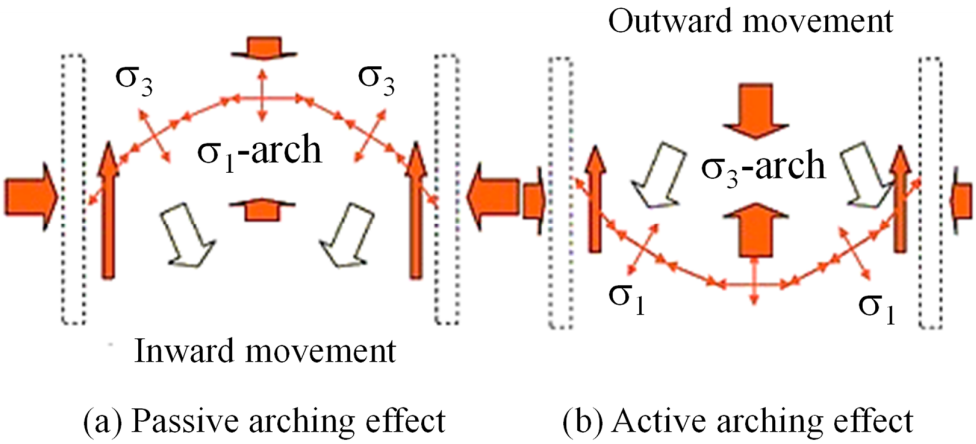

Figure 3. Schematic view of stress distribution of active and passive arching [21].

Active arching occurs when the structure is more compressible than the surrounding soil, and arching can decrease the loads on the structure by as much as 95 percent. Passive arching happens when the soil is more compressible than the structure and arching can increase the loads on the structure by several hundred percent.

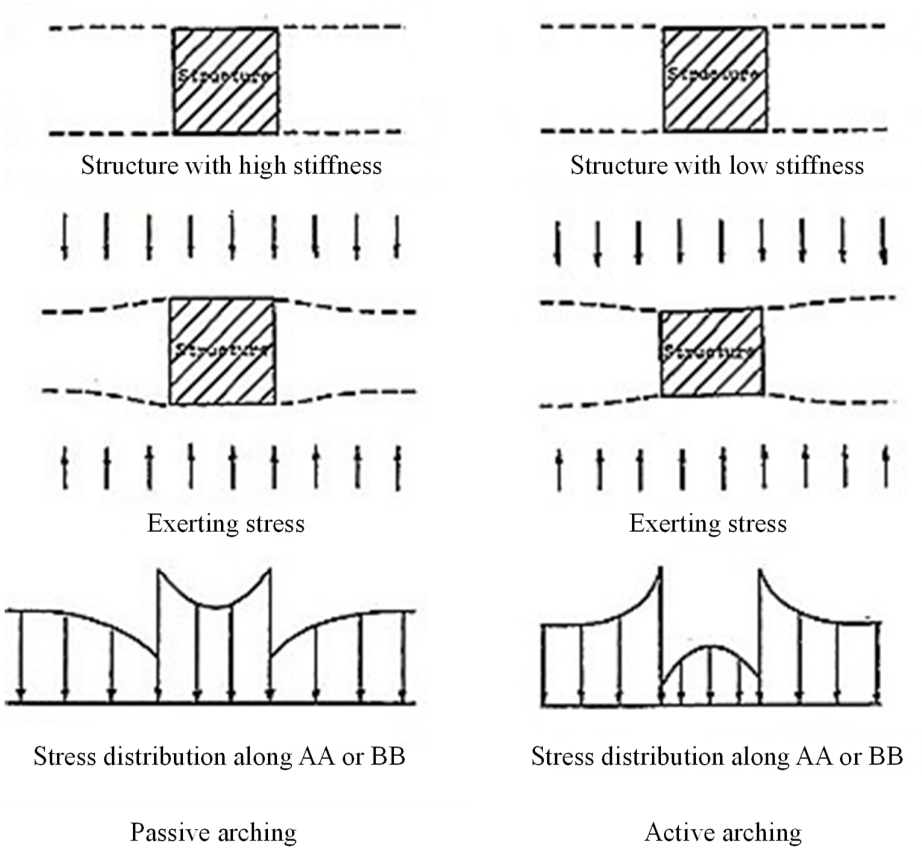

Figure 4. The vertical cross-section of stress redistribution [18].

If the soil mass and the structure have the same constitutive properties, the stress will be uniform. The stress along the vertical direction will be linear and increasing with depth (geostatic stresses) as no arching would appear in this case [18]. Figure 4 shows stress distribution regarding active and passive arching. Underground structures usually do not have uniform deformation. This makes the stress distributions more complex than those discussed above, and the structure may experience active and passive arching simultaneously.

Active soil arching is the prominent phenomenon in geotechnical projects, such as retaining structures under active mode and trapdoors and is widely considered in geotechnical engineering studies [58-63]. On the other hand, the concept of passive soil arching is applicable to some geotechnical projects, such as retaining structures under passive mode, undercut slopes and pile reinforced slopes [64-73]. Some of the arching-based theories for prediction of induced stress distribution around tunnels are reviewed here.

2.1. Terzaghi (1943)

Terzaghi (1943) conducted research on the soil arching phenomenon using a trapdoor experiment testing setup. His test results indicated that when the trapdoor displacement increased, in addition to stress redistribution, the slip surfaces between the stationary and mobilized parts were changed as well. Therefore, Terzaghi (1943) simplified the curved slip surfaces into vertical straight lines, as shown in Figure 5. According to his analysis, the vertical stress on the tunnel can be predicted using the fallowing equation [25].

$$\sigma_v = \frac{B(\gamma - c/B)}{K\tan\varphi}(1-e^{-K\tan\varphi z/B}) + qe^{-K\tan\varphi z/B} \quad (1)$$

where σ_v = vertical stress, B = width of the mobilized portion, c = effective cohesion of soil, φ = effective friction angle of soil, q = surcharge on the ground surface, γ = unit weight of soil, and k = lateral earth pressure coefficient.

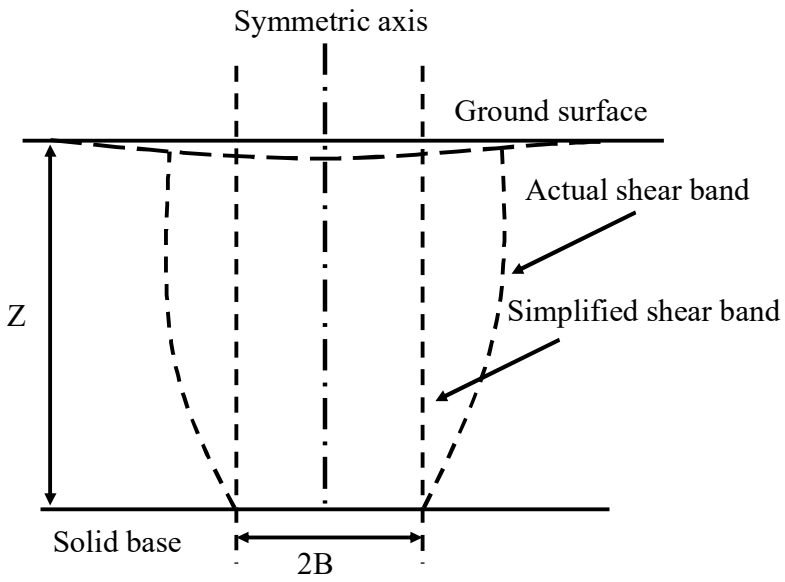

Figure 5. Simplified shear band in sand due to yield of support [25].

Han *et al*. (2017) found that Terzaghi's equation accurately forecasted the pressure when the trapdoor displacement was equal to 10% of the trapdoor width [74]. Therefore, the simplification of Terzaghi's solution led to the estimation of a lower limit of the applied stress on the supports. As a result, many researchers have attempted to improve the Terzaghi's solution.

2.2. Li *et al*. (2013)

Li *et al*. (2013) adopted the Marston (1930) solution to develop a one-dimensional stress field within the deformed zone above the tunnel. As shown in Figure 6, inclined linear slip surfaces between the stationary and mobilized parts are assumed in their analysis [75].

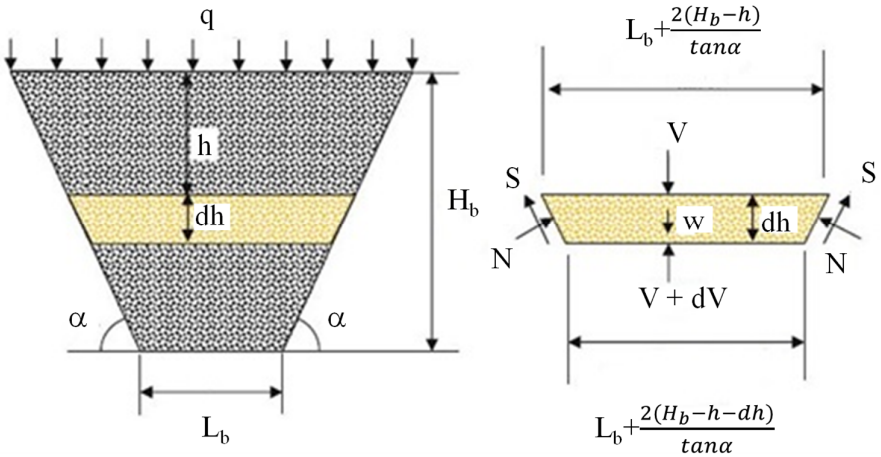

Figure 6. The force distribution inside the deformed zone above a tunnel assumed in Li *et al*. (2013) analysis [75].

The vertical stress above the tunnel, based on the method of Li *et al*. (2013) can be obtained from Equation 2.

$$\sigma_v = \frac{\gamma D}{2(\lambda-1)}\left(1-\frac{2z}{D}\right)\left(1-\left(1-\frac{2z}{D}\right)^{\lambda-1}\right)+q\left(1-\frac{2z}{D}\right)^{\lambda} \quad (2)$$

$$\lambda = K(\tan\alpha\tan\delta+1)-1 \quad (3)$$

$$D = L_b \tan\alpha + 2H_b \quad (4)$$

where σ_v is vertical stress, α, L_b and H_b are the geometrical parameters according to Figure 6 , K is lateral earth pressure coefficient, δ is the interface friction angle between the backfill soil and the slip surface, and γ is the unit weight of soil.

The variation of vertical stress as a function of depth is shown in Figure 7.

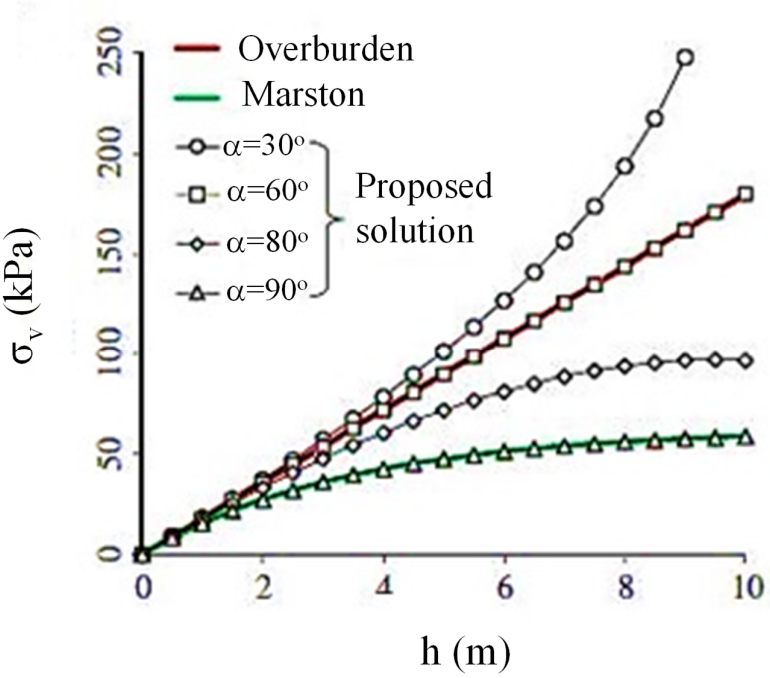

Figure 7. Variation of the vertical stresses for different wall inclination, based on the solution of Li *et al.* (2013) [75].

Figure 7 shows that the vertical stress along the centerline decreases with depth when the wall inclination is equal to 90, and this solution produces stress values identical to those obtained from Marston's solution. When the wall inclination decreases to 60°, the stress increases linearly with depth, and the stress changes are equivalent to geostatic stress conditions. For wall inclinations less than 60°, the value of vertical stress along the centerline increases with increasing depth. This indicates that Li *et al.* (2013) did not consider the effect of soil arching in their solution.

2.3. Khandouzi and Khosravi (2023)

As shown in Figure 8, a two dimensional stress distribution was assumed inside the deformed zone above a tunnel, and the equilibrium equations were solved to develop new solutions [6].

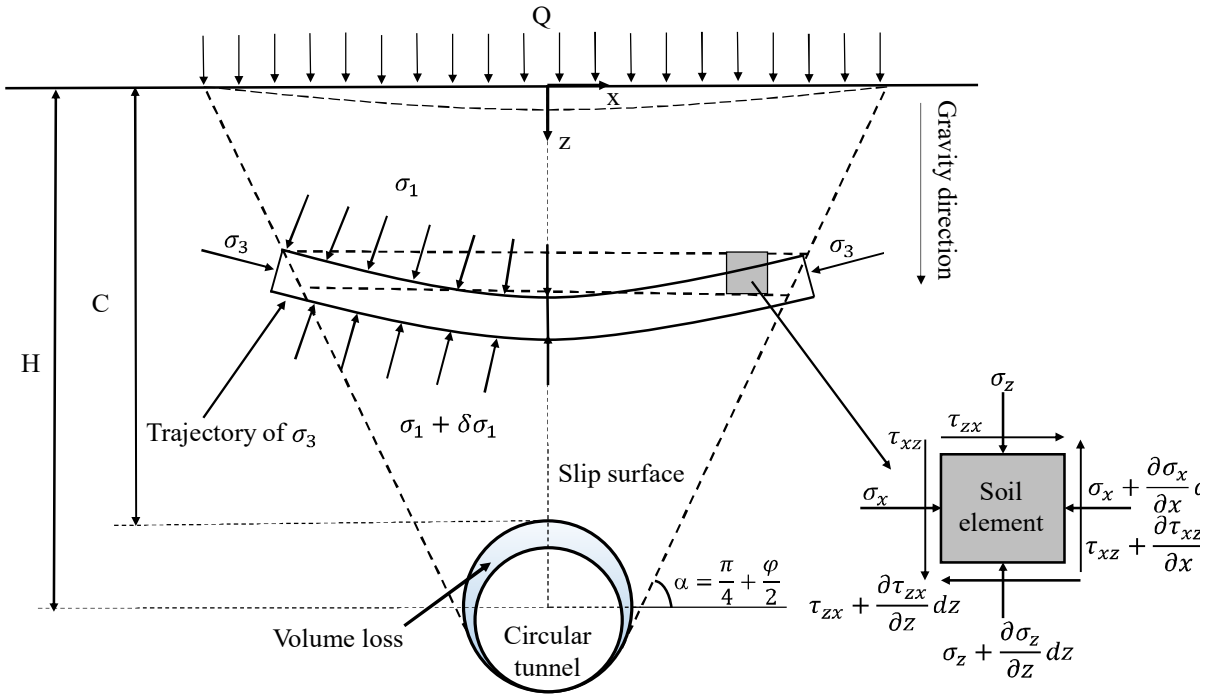

Figure 8. The stress distribution inside the deformed zone above a tunnel in assumed Khandozi and Khosravi (2023) analysis [6].

Figure 9 shows the two-dimensional stress field resulting from their solution. As it is clear from this figure, due to soil arching, the distribution of stresses inside the deformed zone is non-linear. In addition, the shear stress is zero along the vertical symmetric line above the tunnel, and has its maximum value along the shear bands.

Before tunneling, the vertical stress has a triangular distribution. With the excavation and convergence of the tunnel and as a result, the vertical stress distribution becomes non-linear. Figure 10 shows the stress distribution lines before and after arching for a circular tunnel with the radius of R = 3 m at a centerline depth of 25 m.

The point at which the stress distribution curve deviates from the linear state is defined as the depth of arching initiation. The height (H_a) of this point from the tunnel crown presents the upper boundary of the arching zone. The inflection point of vertical stress is stated as the lower boundary of the arching zone. Therefore, the height (H_l) of the loosened zone can be defined as the vertical distance from this point to the tunnel crown as shown in Figure 10 [6].

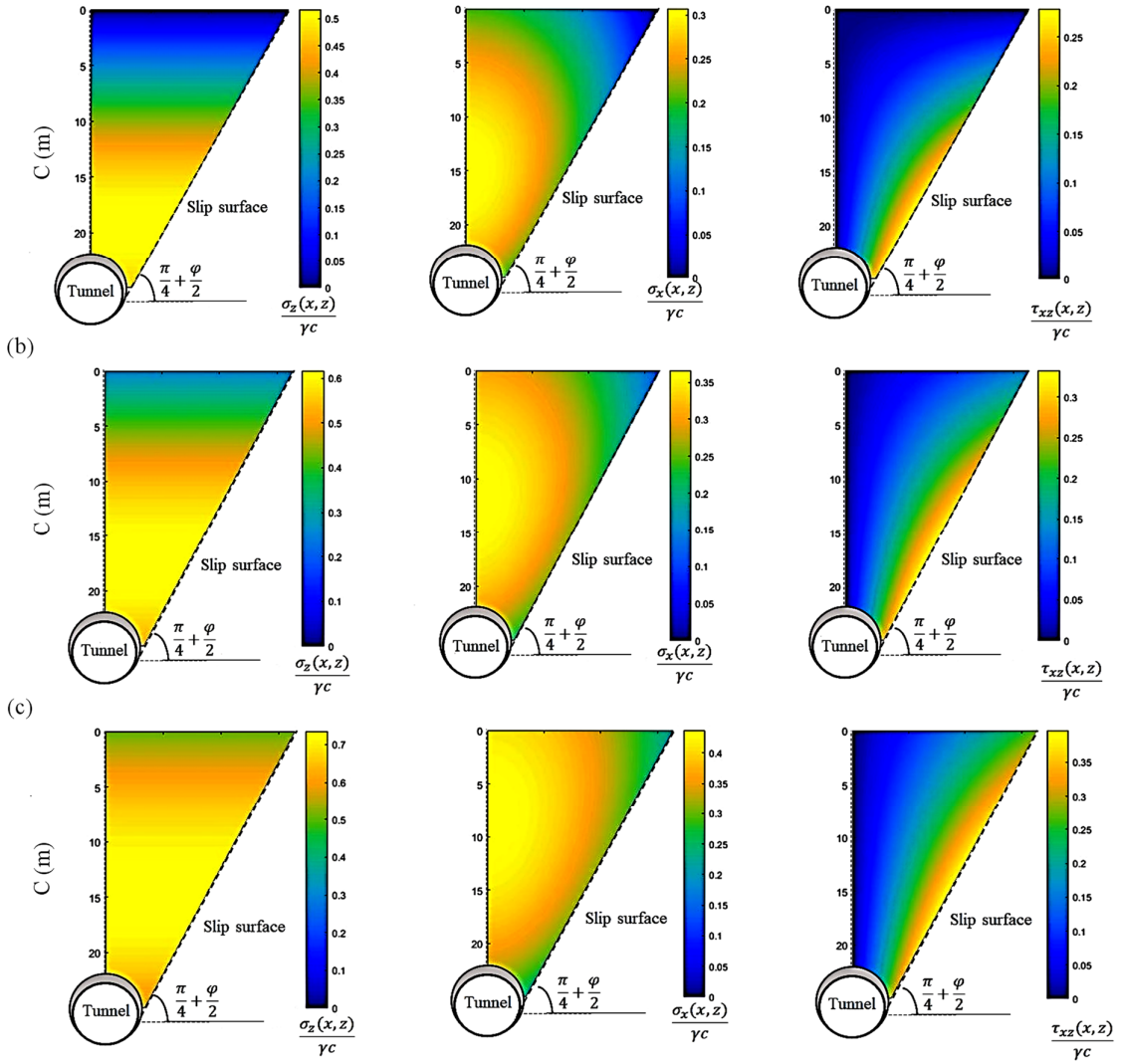

Figure 9. Vertical, horizontal, and shear stress distribution inside the deformed zone above the tunnel [6].

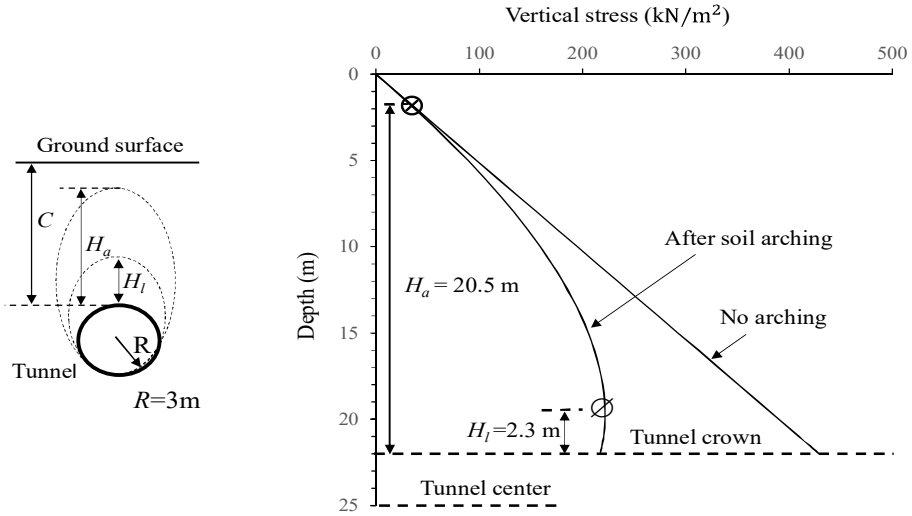

Figure 10. Determination of the arching and loosened zone height from the vertical stress curve [6].

The accuracy of the proposed method was evaluated by comparing the results of the mentioned method with Lin *et al.*'s (2019) numerical data in Figure 11. The analytical solution provided by Terzaghi (1943) and Li *et al.*'s (2013) are also shown in this figure for comparison. According to Figure 11, Terzaghi (1943) underestimates the distribution of earth pressure. Although Li *et al.*'s (2013) solution estimates stress values with a linear distribution, many investigations have shown that due to the arching effect, the pressure distribution is non-linear. The method proposed by Khandozi and Khosravi (2023) shows an acceptable estimated values of earth pressure.

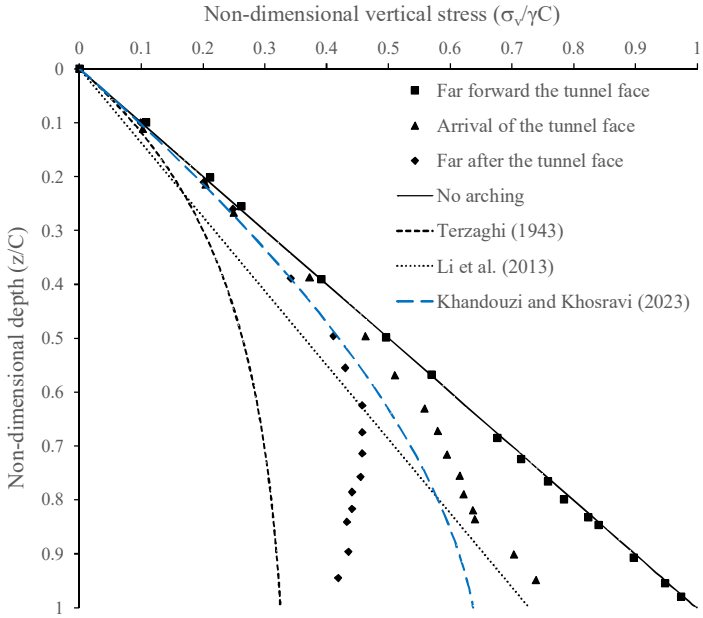

Figure 11. The comparison between the proposed analytical methods and numerical data of Lin *et al.* (2019) [6].

3. Ground Deformation Mechanism

It is important to understand the effect of various factors such as tunnel depth, tunnel volume loss, loading conditions, surcharge, and geo-material type on ground deformation, stress field, strain field, displacement, shear strain, formation and development of slip surfaces or shear bands, and the shape of the settlement trough. In the late 1970s, extensive studies and research were conducted on the phenomenon of soil arching using different approaches and methods with various experimental setups such as the trapdoor test. Additional experiments were carried out that showed a new path and direction relating to the study of this phenomenon in soil environments. A research group at Cambridge University conducted a series of tests to examine the behavior of shallow tunnels in soft grounds under the supervision of Atkinson (1977). They used a geotechnical centrifuge machine to conduct experimental tests [76]. This section reviews some of the experimental studies regarding ground deformation and presents a comprehensive explanation on the effect of the above-mentioned factors on ground deformation and soil arching around tunnels because of its importance.

3.1 Costa *et al.* (2009)

Costa *et al.* (2009) investigated the mechanism of failure and formation of shear bands for shallow conditions. The primary nonlinear slip surfaces of OA start from the corners of the trap door and continue inward to the symmetric axis as shown in Figure 12. The angle formed between the vertical and the tangent at any point along shear band OA equals the soil dilatancy angle that corresponds to the stress level. When the trapdoor moves down, a new shear band is created in the soil (slip surface OB). Surface OB in Figure 12 has a smaller dilatancy angle than surface OA because when primary shear band OA or slip surface is formed, soil density decreases, and results in a lower soil dilatancy angle for new slip surface OB [48].

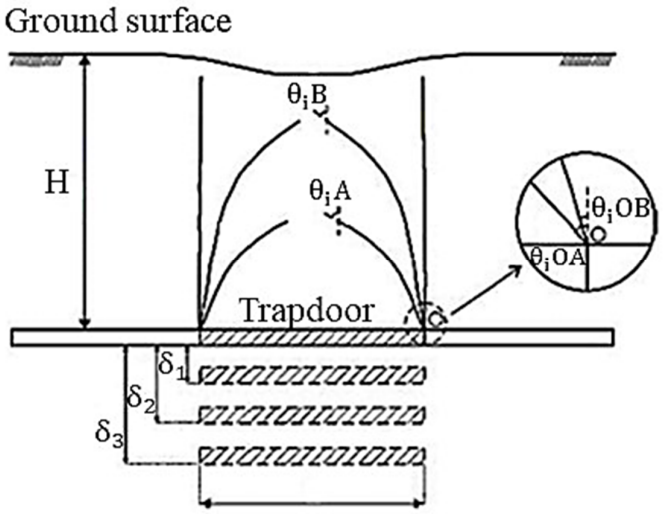

Figure 12. The deviation of slip surfaces with trapdoor test displacement undel shallow condition [48].

For deep condition, Zhao *et al*. (2021) illustrated the development of shear bands as shown in Figure 13.

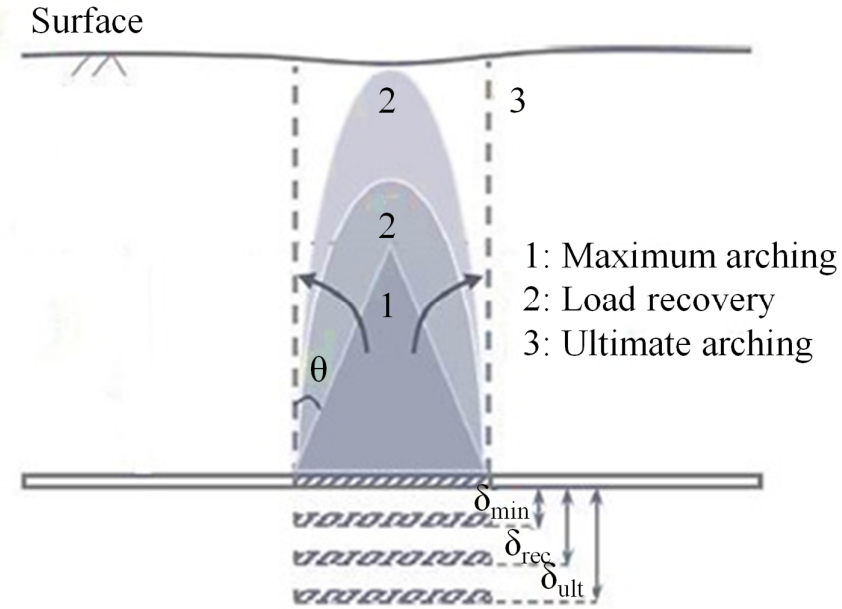

Figure 13. The progressive development of the shear bands under deep condition [47].

According to Figure 13, Zhao *et al*. (2021) presented that θ is equal to the dilatancy angle based on the experimental results under deep conditions. This is different from the internal friction angle which was concluded by Iglesia *et al*. (2013) or $\pi/4 - \phi/2$ for shear bands as recommended by Rui *et al*. (2016) [47, 77]. Zhao *et al*. (2021) also compared the process of development and formation of shear bands with increasing displacement for shallow and deep conditions. He indicated that the development and formation of shear bands are similar for deep and shallow tests. However, there is a difference between the two tests in that the shear bands are joined to each other in deep tests but will not intersect with each other in shallow conditions [47].

3.2. Marshall (2009)

Marshall (2009) conducted a study on the behavioral mechanism of the sand environment due to tunnel convergence using a geotechnical centrifuge constructed at the Cambridge University [78]. By performing various tests using Digital Image Correlation (DIC) technique and recording settlement with Linear Variable Differential Transformer (LVDT), Marshall presented the behavioral mechanism of the sand environment. The shear bands and deformation zones above a circular tunnel for different values of tunnel volume loss is shown in Figure 14.

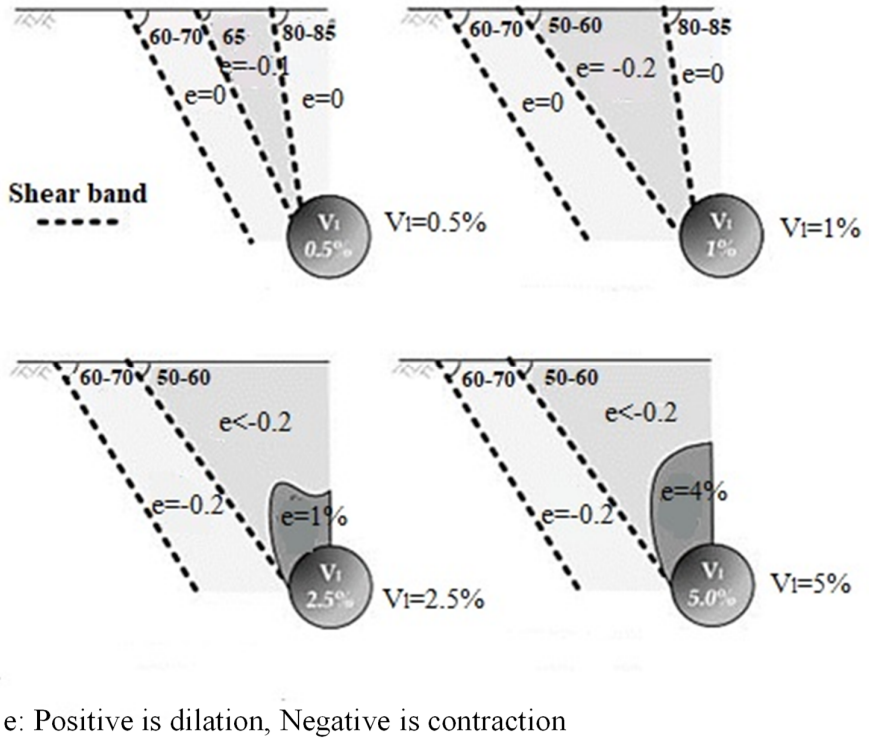

Figure 14. Observed displacement mechanism by Marshall (2009) [78].

According to Figure 14, at low tunnel convergences (0.5 to 1%), the soil within a chimney-shaped zone above the tunnel displaces vertically downwards as a rigid body without showing signs of volumetric change. At 2.5%, the settlement trough grows, and the soil above the tunnel, which is in a state of contraction, begins to expand. The dilation zone forms above the tunnel. In this case, the extent of the settlement trough is not similar to that at tunnel convergence from 0.5 to 1%. The results of the laboratory tests of the tunnel model at 2.5% indicate that the initiation of the dilation zone above the tunnel may be coincident with the end of the growth of the width of the settlement trough. At 5% volume loss, conditions are similar to those at 2.5%, except that the size and magnitude of the dilation zone have grown.

Marshall (2009) introduced the formation and development of expansion and contraction zones above the tunnel crown as a proof for the difference between the tunnel volume loss and the ground volume loss on the ground surface based on the experimental results [78].

3.3. Zhou (2014)

The geotechnical centrifuge model of Marshall (2009) was later modified by Zhou (2014), as shown in Figure 15. Zhou (2014) used two digital cameras to capture images of sand behind the plexiglass window during the test to measure the displacement. The cameras were positioned carefully to capture the whole soil above the tunnel model during the tunnel volume loss at the same time. In this method, a set of fluorescent lights were positioned carefully in front of the window to minimize reflection from plexiglass. The images were analyzed using PIV utilities to map the movement of soil in terms of pixel movements. First, the picture of the soil taken before tunnel

volume loss initiation was imported into the software, and the grid were traced to create a template file. The images taken during the tests were imported into the template file. The measurement of the distances between the template grid and the image grid obtained the displacements at different position in the soil [79].

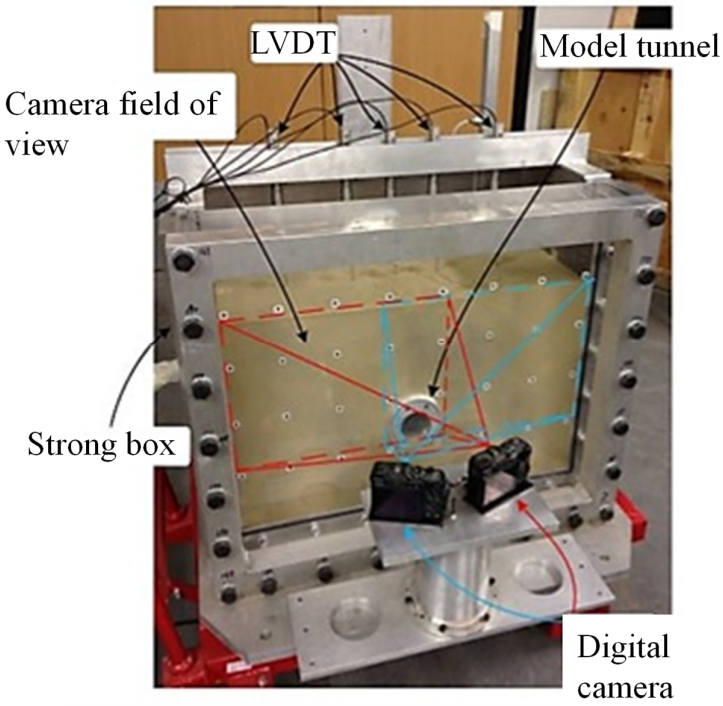

Figure 15. The centrifugal experimental setup used by Zhou (2014) [79].

Zhou (2014) conducted studies on the behavioral mechanism of the sand environment around circular tunnels, the formation of shear bands and expansion zones, and the effect of density on the displacement field. Concerning the effect of soil density on the volume strain, Zhou (2014) obtained results based on Figure 16.

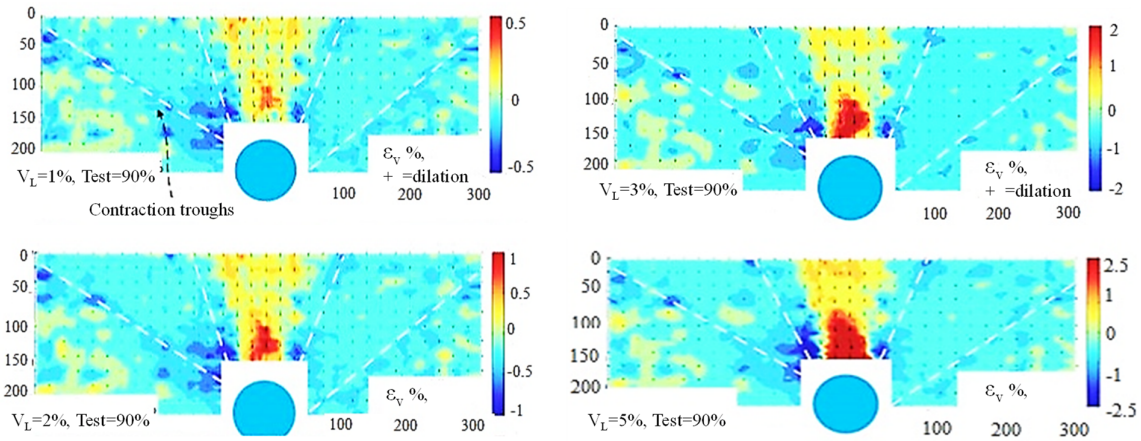

Figure 16. Volume strain contours for different tunnel volume loss [79].

At a low volume loss of 1%, two main semi-vertical shear bands extend from the tunnel shoulders towards the ground surface. The chimney-shaped zone between shear bands does

not show large volumetric change. At a medium volume loss of 2%, the shear bands are more evident. The dilation of the sand environment is greater, which is associated with the localization of displacement above the tunnel crown. At a volume loss of 3%, there isn't much development of shear bands, and the expansion zone is concentrated at the tunnel crown. At an extremely high volume loss of 5%, such a similar situation also continues for tunnel convergence up to 5%. As a general conclusion, Zhou (2014) stated that with the increase of tunnel convergence from 1% to 5%, the extent of shear bands decreases, and the localization of the expansion zone at the top of the tunnel crown becomes more evident [79]. It is clear that the initiation of the expansion zone above the tunnel is coincident with the end of growth of the settlement trough.

3.4. Franza (2016)

Due to the complex behavior mechanism of the sandy environment, Franza (2016) conducted a comprehensive study to investigate the various effects on the settlement trough and displacement field. Franza (2016) investigated the C/D and density effect on settlement contours, displacement field, and shear strain for models with relative densities of 30%, 50%, 70%, and 90% and C/D values equal to 1.3 and 6.3. The several results obtained by Franza (2016) are described in Figure 17 and Figure 18.

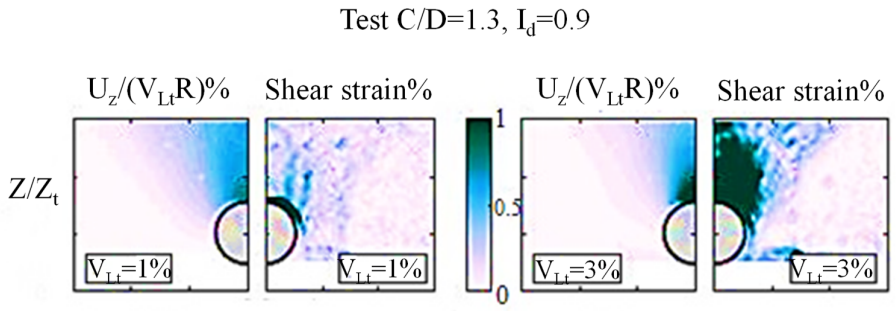

Figure 17. A sample of settlement contours and shear strain in concentrated sand [80].

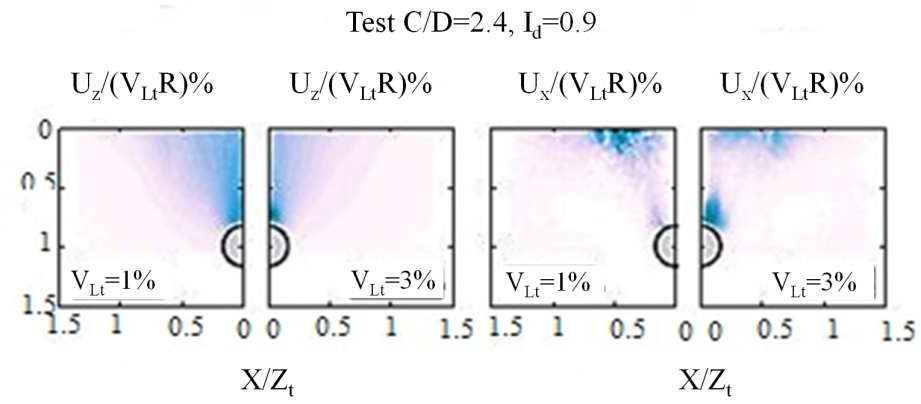

Figure 18. A sample of vertical and horizontal displacement contours [80].

Based on the Figure 17, Figure 18, and additional experimental results, Franza (2016) summarized the displacement mechanism in Figure 19 that showed the effect of C/D and density on the ground deformation. According to Figure 19, it appears that the soil arching phenomenon plays an important role in defining tunneling-induced displacement mechanisms, and it can help to explain (1) the transition from a chimney-like displacement field to a wide displacement field with increasing C/D, (2) The narrowing and limiting of the displacement field with tunnel convergence, and (3) the complex variation of settlements with soil density [80].

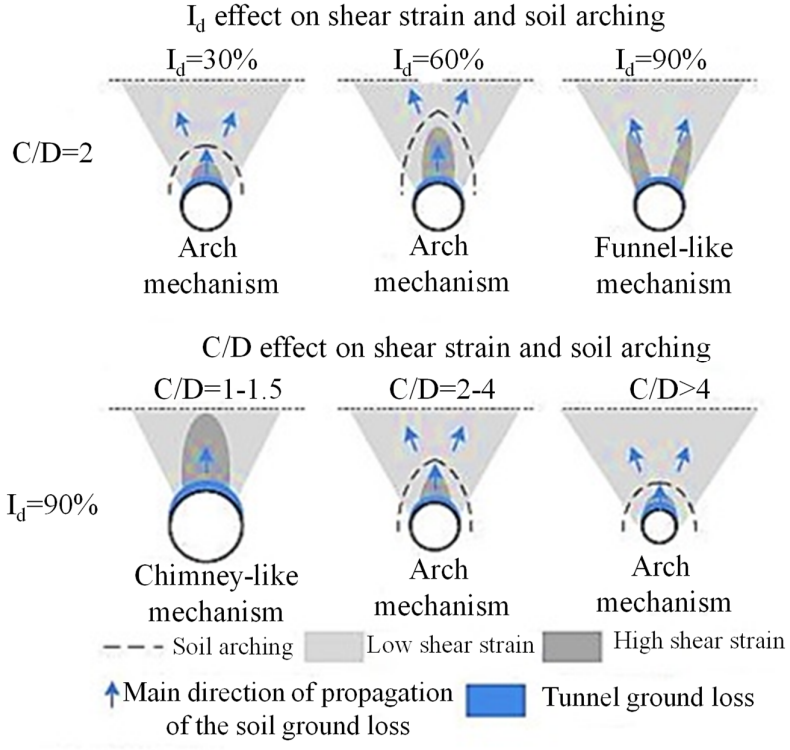

Figure 19. The influence of C/D and relative density on soil strain and the arching mechanism [80].

3.5. Zhang *et al.* (2016)

Zhang *et al.* (2016) investigated the effect of trapdoor displacement on the development of sliding surfaces based on Terzaghi's (1943) arching model as shown in Figure 20. Shearing bands progress from the corners of the trap-door at inward oblique curves to the vertical direction as trap-door displacement increases from several to dozens of millimeters, and then to outward oblique lines as shown in Figure 21 [51]. The inclination of slip surfaces decreases from 90 to 45 + φ/2 from horizontal direction as overburden height increases [25].

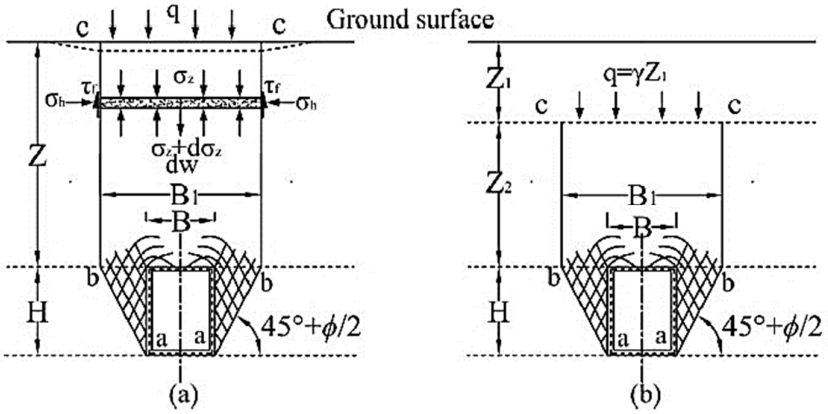

Figure 20. Schematic representation of Terzaghi arching model (a) Arching model I, (b) Arching model II [51].

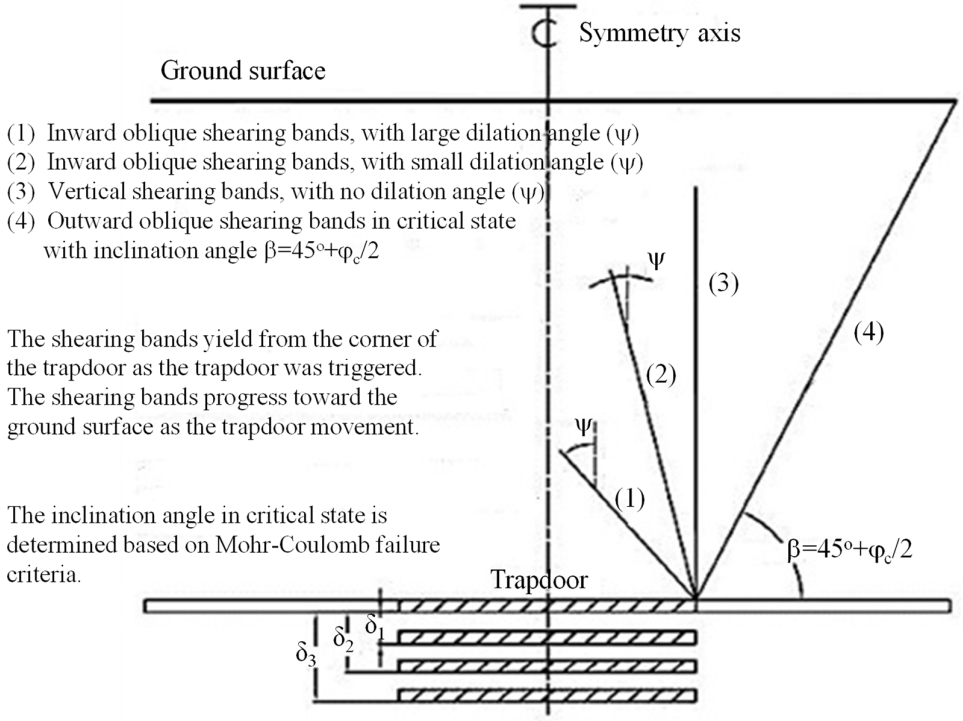

Figure 21. Shear band development mechanism in trapdoor setup [51].

There is difference between these two arching models, as shown in Figure 20. In model I, the slip surfaces reach the ground surface and the settlement is clear. In model II, the slip surfaces do not develop to the ground surface, so the deformation is replaced by the contraction and extension zones above the tunnel. The difference in the development of slip surfaces causes a considerable change in the load exerted on underground structures [51]. Figure 22 shows changes in stress in the vertical direction for two types of arching models.

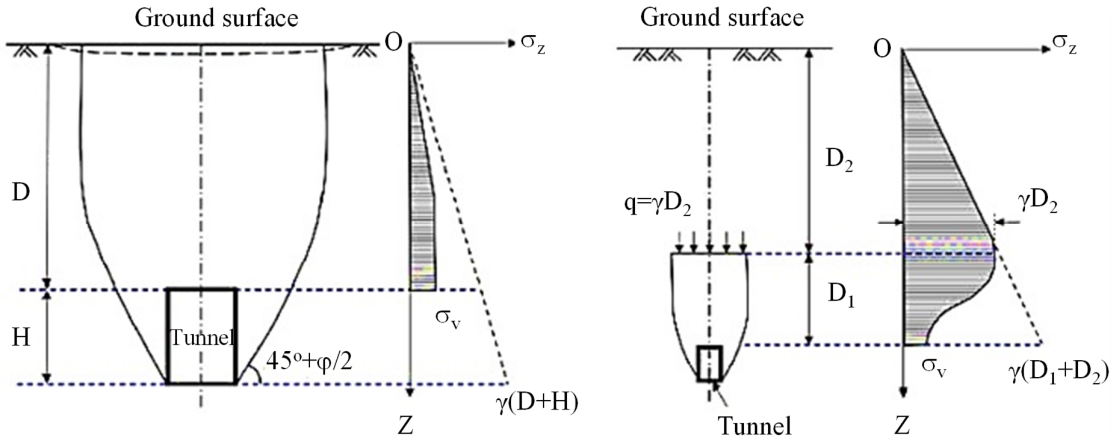

Figure 22. Vertical stress profile at centerline after tunnel excavation [16].

Following Terzaghi's studies, Zhang *et al*. (2016) illustrated that the vertical stress calculated by the arch model (II) is between the arch model (I) and the geostatic stress, which can be introduced as the upper and lower limits of stress changes. A design based on the upper limit is conservative but may not be economical, whereas a design based on the lower limit is economical but may be unsafe [51].

3.6. Khatami (2018)

Khatami (2018) studied the effect of geo-material type, loading condition and surcharge on the shape and inclination of shear bands. The inclination of shear bands is significantly influenced by loading conditions including active and passive. Figure 23 shows that passive slip surfaces are oriented outwards while active slip surfaces are inclined inwards. The results also show that the deformed zone is symmetric for two tests and that the passive deformed zone limiting with slip surfaces is larger than the active deformed zone [81].

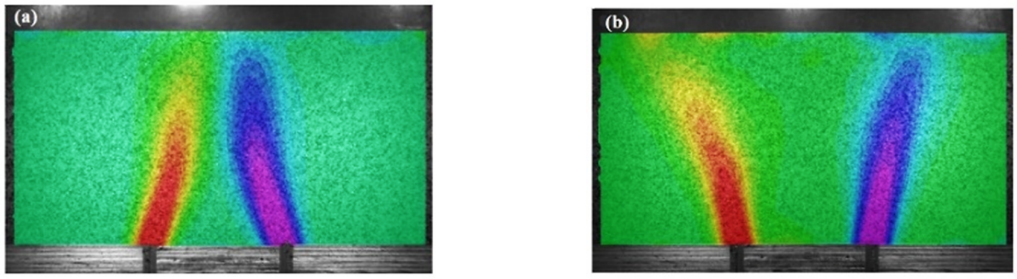

Figure 23. The effect of testing type on slip surfaces (a) active test, (b) passive test [81].

Figure 24 indicates the effect of surcharge on the angle of slip surfaces. According to this figure, surcharge leads to a changes in the angle of slip surfaces and the development of expansion and contraction zones in the sand environment.

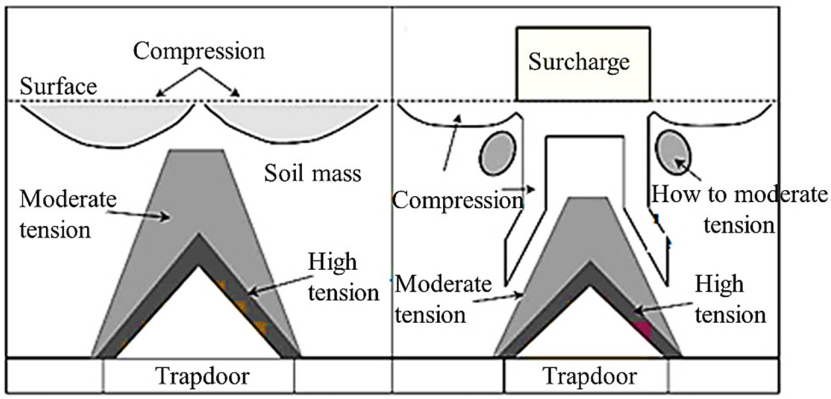

Figure 24. The influence of surcharge in the appearance of expansion and contraction zones above a trapdoor [81].

The type of used geo-material affects the shape of slip surfaces that limit the boundary of the deformed zone. Figure 25 shows the experimental test results using sand materials and a rubber-sand mixture. According to this figure, the rubber-sand mixture changes the slip surfaces at the boundary of the deformed zone from a triangular to a curved shape. Furthermore, the presence of rubber is effective in developing the deformed zone, applying stress on the trapdoor test, and settling on the ground surface. When there is an increase in the amount of rubber in the sandy environment, settlement and deformed zone height decrease, and the pressure exerted on the trapdoor reduces [81].

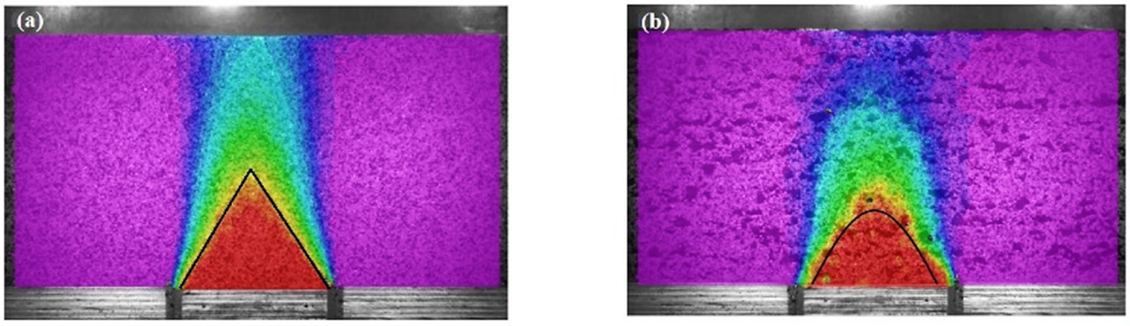

Figure 25. (a) The triangular arch for sandy soil, (b) The curved arch for rubber-sand mixture [81].

3.7. Moussaei *et al*. (2019)

Moussaei *et al*. (2019) developed a new physical modeling setup for simulation of full-face tunnel excavation, using a pack of conic wedges, illustrated in Figure 26. A permanent magnet step motor with no vibration was used to control the tunnel volume loss. The behavioral mechanism of the sand medium was studied by image processing and earth pressure measurement throughout the tunnel convergence. The effect of tunnel convergence, tunnel depth, and soil density on the ground deformation were investigated in their study.

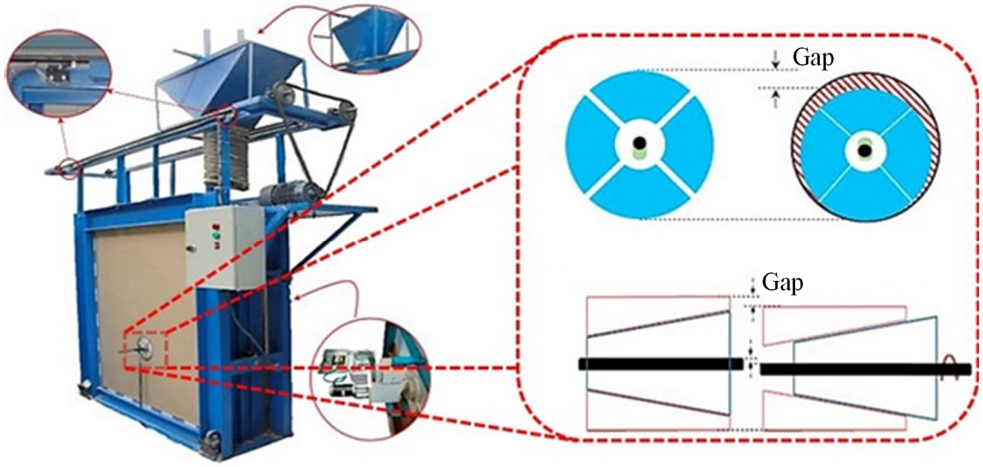

Figure 26. The physical model setup developed by Moussaei *et al*. (2019) [82].

According to the test results for a cover to diameter ratio of C/D = 3 shown in Figure 27, as the tunnel volume loss increased, the ground near the tunnel crown deformed and the boundary between the deformed zone and the surrounding stationary zones became more clear. Additionally, as the soil density increased, the deformed area was more limited to the tunnel crown [82].

3.8. Song *et al.* (2020)

Song *et al*. (2020) investigated the effect of the tunnel model type on the behavioral mechanism of the sand environment. The flexible membrane (FM) model tunnel used by Marshall (2009), Zhou (2014), and Franza (2016) was replaced by a rigid boundary mechanical (RBM) model in his investigation, shown in Figure 28

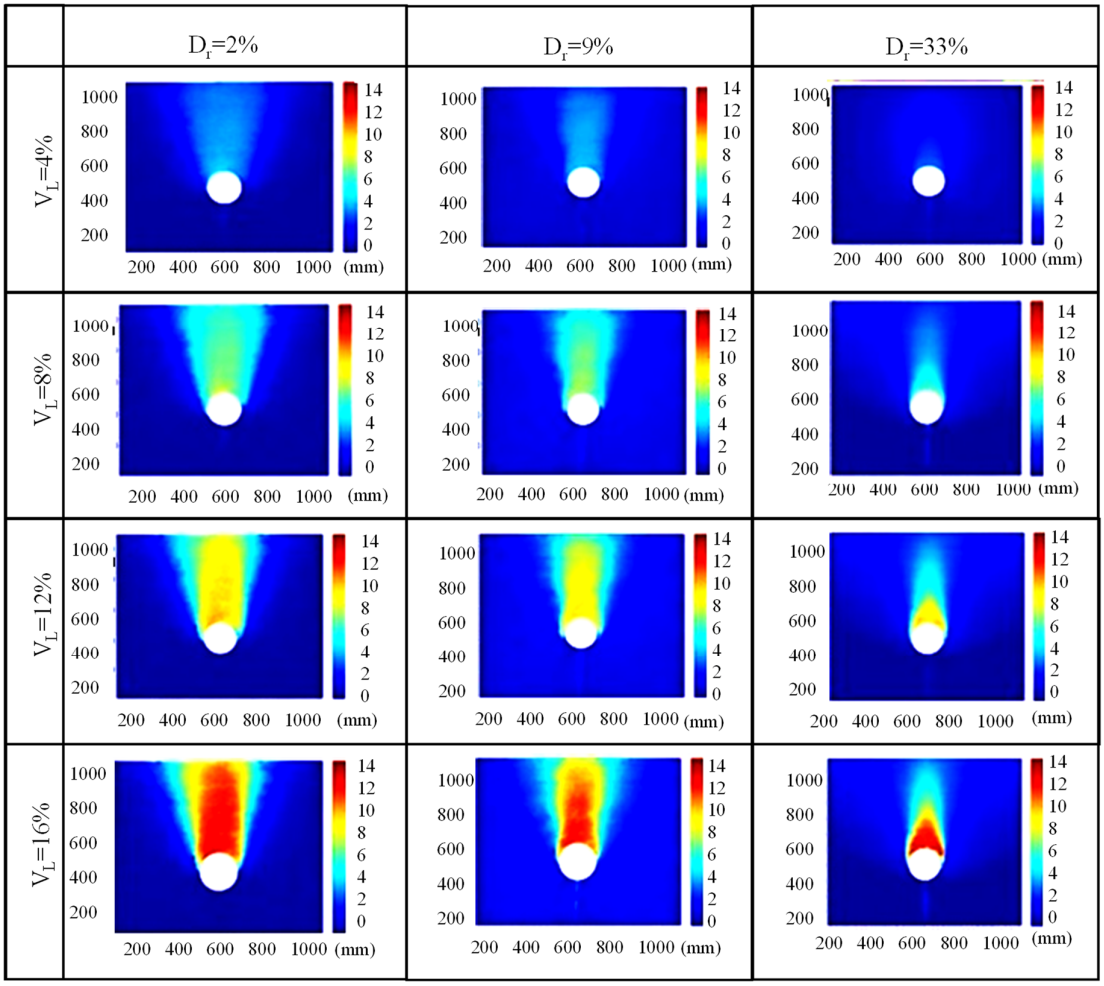

Figure 27. Ground deformation during tunnel convergence for C/D = 3 [82].

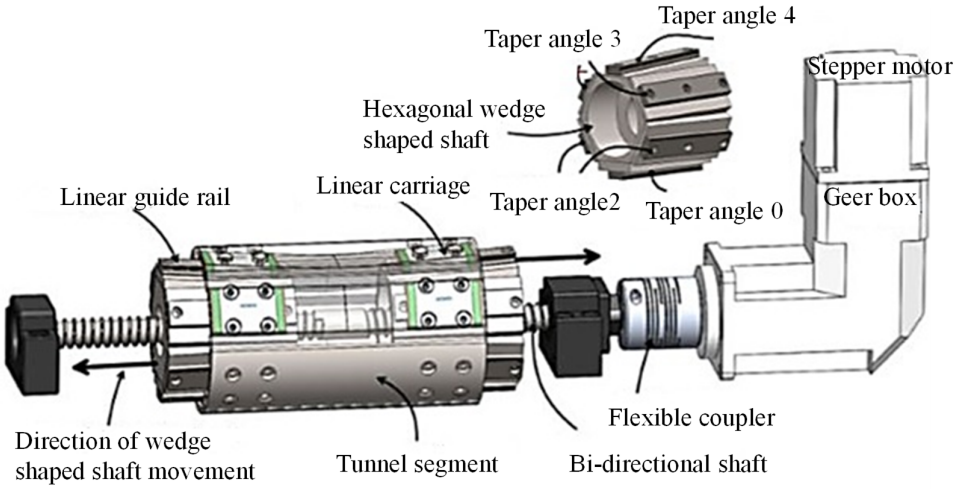

Figure 28. An eccentric rigid boundary mechanical (RBM) model tunnel [83].

The construction of this tunnel model aimed to produce non-uniform radial displacements around the tunnel, causing maximum soil displacements at the tunnel crown. Song *et al*. (2020) compared the size of the expansion area and shear strains for two tunnel models. Figure 29 shows the comparison result for those models. The comparison shows that an eccentric rigid boundary mechanical (RBM) model tunnel allows the formation of larger shear strains in the sand environment for similar volume loss. Thus, the high shear strain will result in a greater volumetric expansion for the mechanical tunnel model [83].

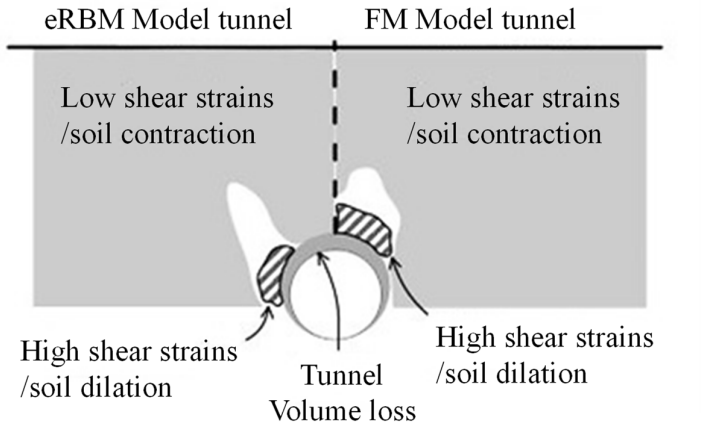

Figure 29. Comparison of expansion zones and shear strains for two different tunnel models [83].

4. Discussion

This paper reviewed research that has investigated specific parts of the formation and development of shear bands, ground deformation, and the effect of different factors on it. However, no comprehensive information has been provided regarding the relationship between shear bands, the shape and development of the deformed area, the arching effect, and its effect on stress redistribution.

Regarding the shear bands, the shape and development of the deformed area can be referred to Wu *et al.* (2019) and Long and Tan (2020)'s research results. Using the trapdoor test results and the theory of gravity flow of granular materials described by Janelid and Kapil (1966), Wu *et al*. (2019) considered the shape of the deformed zone as ideally elliptical [84, 85]. Wu *et al*. (2019) compared their research output with Lee *et al*. (2004), Lee *et al*. (2006), and Shahin *et al*. (2007) according to Figure 30, and concluded that the assumption of an ideal elliptical shape for the deformed zone is in good agreement with the laboratory results of other researchers [85].

Long and Tan (2020) investigated the soil leaking of the tunnel, experimentally. They compared the experimental results with Janelid and Kapil's theory (1966). They concluded that the shape of the deformed zone caused by tunnel leakage or the tunnel convergence at the top of the tunnel can be defined as an ellipse [89].

Regarding the phenomenon of soil arching and its effect on stress redistribution can be referred to Iglesia *et al*. (2013) and Franza (2016) studies and other researchers. According to Figure 31, there is a significant relationship between the occurrence of soil arching, stress redistribution, and the development of deformed zones.

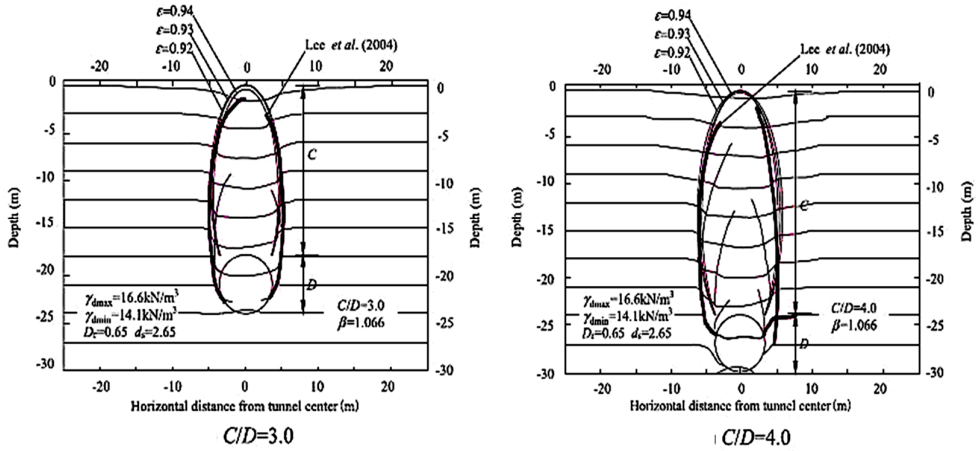

Lee *et al*. (2004)

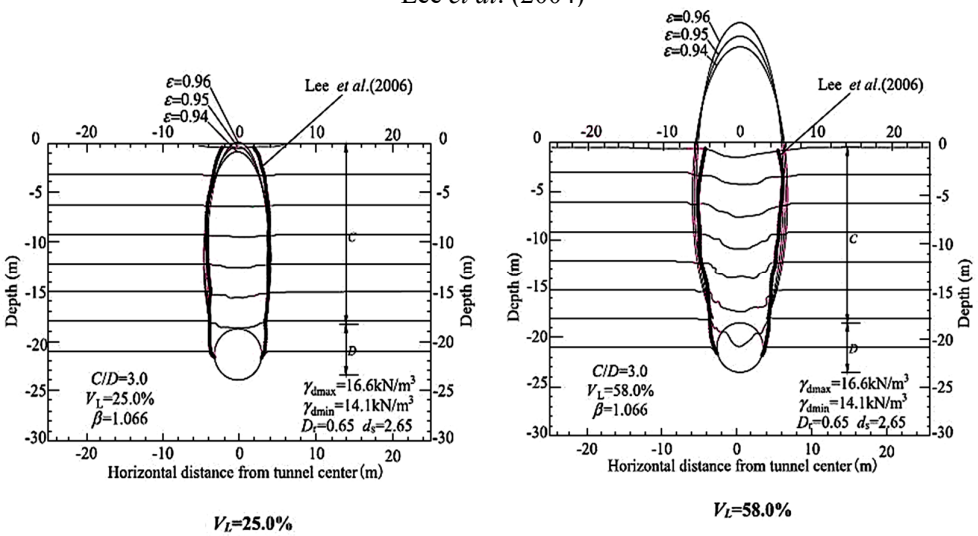

Lee *et al*. (2006)

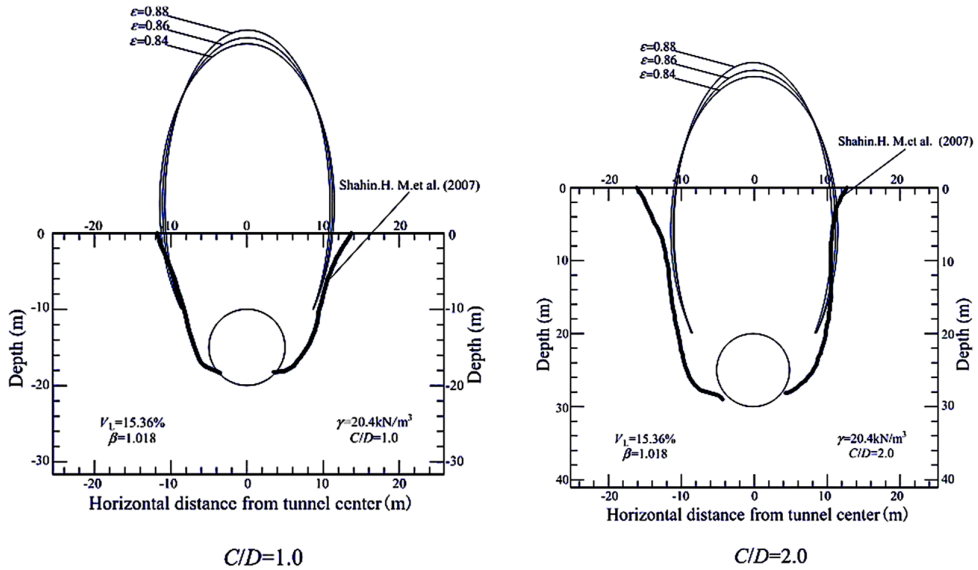

Shahin et al. (2007)

Figure 30. The comparison of Wu *et al.* (2019) results with Lee *et al.* (2006), Lee *et al.* (2004), and Shahin *et al.* (2007) [86-88].

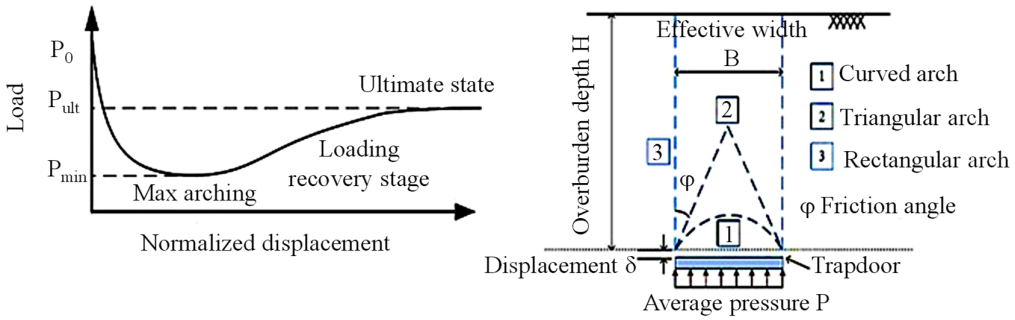

Figure 31. The load-displacement curve and the development of stress arching above a trapdoor [50, 80].

According to Figure 31, it can be concluded that with the onset of tunnel convergence or trapdoor displacement, a curved shear band (1) initiate from the tunnel shoulder or trapdoor corner and continue in an inward orientation toward the ground surface. These shear bands and primary slip surfaces separate the stable area from the deformed zone. Increasing the tunnel convergence activates the shear resistance between the deformed zone and the surrounding stable areas. In this case, the stress field in the moving zone changes and causes the formation of the first stable arch. The primary stable arch causes a sudden drop in the applied load on the model. This condition corresponds to the minimum point in the load-displacement graph of the trapdoor test. The increase in the tunnel convergence or trapdoor displacement destroys the first stable arch and causes the arching zone to grow and stable arches to form at distances farther from the trapdoor. This situation leads to exerting more loads on the trapdoor. The mentioned situation is related to the stage of load recovery in the load-displacement curve and the formation of a triangular arch (2) above the trapdoor. If a stable arch is formed above the trapdoor, the development of the loosened zone is stopped, and the load exerted on the trapdoor doesn't change. If a stable arch is not formed by increasing the trapdoor displacement, then the shear band will grow and coincide with the rectangular arch (3) which results in an increase of the load because of more volume of ground without support.

5. Conclusions

The excavation of underground spaces usually results in convergence of the cavity and ground volume loss, leading to the formation of shear bands or slip surfaces around the cavity, the development of the deformed zone, and stress redistribution. This review explains soil arching and stress redistribution, slip surfaces and factors influencing them, and ground deformation mechanisms in sandy environments. According to the reviewed studies, the following results can be obtained:

- The research confirms that shear bands, ground deformation, soil arching, and stress redistribution are related to each other.
- Primary shear bands form when the tunnel converges or model displaces. These bands separate the deformed zone from the stable area.
- With an increase in convergence, shear stress on the slip surfaces is activated, and causes a stable arch to form the arching area. This stable arch transfers load from the deformed zone to the stable portion.
- If convergence is high, the stable arch is destroyed and formed at far distances, and a loosened zone develops. This causes more load on tunnels or models.
- If a stable arch forms with convergence or displacement, the amount of applied load on support is constant. Otherwise, the shear band will extend to the surface of the model and increase applied load on the crown of tunnels or models.

The material reviewed in this research will be very useful for engineers who evaluate the redistribution of stress and load on tunnel supports. Future research can focus on developing new methods to predict shear band formation and deformation mechanisms in different types of soil environments.

Declaration of Interests

The authors declare that they have no known competing financial interests or personal relationships that could have appeared to influence the work reported in this paper.

This research work did not receive any specific grant from funding agencies in the public, commercial, or not-for-profit sectors.

References

[1]. Wang, L., Zhang, P., Golewski, G., & Guan, J. (2023). Editorial: Fabrication and properties of concrete containing industrial waste. *Front Mater, 10*, 1169715.

[2]. Golewski, G.L. (2023). Concrete composites based on quaternary blended cements with a reduced width of initial microcracks. *Applied Science*, 13(12), 7338.

[3]. Golewski, G.L. (2023). Combined effect of coal fly ash (CFA) and nanosilica (nS) on the strength parameters and microstructural properties of eco-friendly concrete. *Energies, 16(1)*, 452.

[4]. Golewski, G.L. (2023). Study of strength and microstructure of a new sustainable concrete incorporating pozzolanic materials. *Structural engineering and mechanics, 86(4)*, 431-441.

[5]. Golewski, G.L. (2022). The Specificity of shaping and execution of monolithic pocket foundations (PF) in hall buildings. *Buildings, 12(2)*, 192.

[6]. Khandouzi, G., & Khosravi, M.H. (2023). An analytical investigation of soil arching induced by tunneling in sandy ground. *Tunneling and Underground Space Technology, 140*, 105242.

[7]. Chen, R.P., Song, X., Meng, F.Y., Wu, H.N., & Lin, X.T. (2022). Analytical approach to predict tunneling-induced subsurface settlement in sand considering soil arching effect. *Computers and Geotechnics, 141*, 104492.

[8]. Pabodha, K.K., Kannangara, M., Ding, Z., & Zhou, W.H. (2022). Surface settlements induced by twin tunneling in silty sand. *Underground Space, 7*, 58-75.

[9]. Meng, F.Y., Chen, R.P., Liu, S.L., & Wu, H.N. (2021). Centrifuge modeling of ground and tunnel responses to nearby excavation in soft clay. *Journal of Geotechnical and Geoenvironmental Engineering, 147(3)*, 04020178.

[10]. Wang, F. (2021). Empirical evidence for estimation of subsurface settlement caused by tunneling in sand. *Underground Space, 6*, 577-584.

[11]. Hu, X.Y., He, C., Peng, Z.Z., & Yang, W.B. (2019). Analysis of ground settlement induced by Earth pressure balance shield tunneling in sandy soils with different water contents. *Sustainable Cities Society, 45,* 296–306.

[12]. Franza, A., Marshall, A.M., & Zhou, B. (2018). Greenfield tunnelling in sands: the effects of soil density and relative depth. *Géotechnique, 69(4)*, 297-307.

[13]. Chen, K.H., & Peng, F.L. (2018). An improved method to calculate the vertical earth pressure for deep shield tunnel in Shanghai soil layers. *Tunneling and Underground Space Technology, 75*, 43-66.

[14]. Cheng, H.Z., Chen, J., & Chen, G.L. (2019). Analysis of ground surface settlement induced by a large EPB shield tunnelling: a case study in Beijing, China. *Environmental Earth Science, 78*, 605.

[15]. Lu, D.C., Lin, Q.T., Tian, Y., Du, X.L., & Gong, Q.M. (2020). Formula for predicting ground settlement induced by tunnelling based on Gaussian function. *Tunneling and Underground Space Technology, 103*, 103443.

[16]. Lin, X.T., Chen, R.P., Wu, H.N., & Cheng, H.Z. (2019). Three-dimensional stress-transfer mechanism and soil arching evolution induced by shield tunneling in sandy ground. *Tunneling and Underground Space Technology, 93*, 103104.

[17]. Chen, C.N., Huang, W.Y., & Tseng, C.T. (2011). Stress redistribution and ground arch development during tunneling. *Tunneling and Underground Space Technology, 26*, 228-235.

[18]. Evans, C.H. (1984). An examination of arching in granular soils. *Massachusetts Institute of Technology*, 235p.

[19] Khosravi, M.H., Pipatpongsa, T., & Takemura, J. (2016). Theoretical analysis of earth pressure against rigid retaining walls under translation mode. Soils and Foundations, 56(4), 664-675.

[20]. Xie, Y., & Leshchinsky, B. (2016). Active earth pressures from a log-spiral slip surface with arching effect. *Géotechnique, 6 (2)*, 149-155.

[21]. Khosravi, M.H., Bahaaddini, M., Kargar, A.R., & Pipatpongsa, T. (2018). Soil arching behind retaining walls under active translation mode: review and new insights. *International Journal of Mining and Geo-Engineering, IJMGE, 52(2)*, 131-140.

[22]. Tangjarusritaratorn, T., Miyazaki, Y., Sawamura, Y., Kishida, K., & Kimura, M. (2022). Numerical investigation on arching effect surrounding deep cylindrical shaft during excavation process. *Underground Space, 7*, 944-965.

[23]. Tien, H.J. (1996). A literature study of the arching effect. *Civil engineering, National Taiwan University, Massachusetts institute of technology*, 196p.

[24]. Jakobson, B. (1958). On pressure in silos. *Proc, Conference on Earth Pressure Problems, Brussels*, pp. 49-54.

[25]. Terzaghi, K. (1943). Theoretical soil mechanics. *John wiley & Sons, Inc, New York & London*, 526p.

[26]. Spangler, M.G., & Handy, R.L. (1973). Loads on underground conduits. *Soil Engineering, 3rd Edition, Harper Collins, New York*, pp. 658-686.

[27]. Whitman, R.V., Getzler, Z., & Hoeg, K. (1963). Tests upon thin domes buried in sand. *Journal of the Boston Society of Civil Engineers*, pp. 1-22.

[28]. Luscher, U., & Hoeg, K. (1965). The action of soil around buried tubes. *Proc, Sixth International Conference on Soil Mechanics and Foundation Engineering, Montreal, Canada*, pp. 396-400.

[29]. Getzler, Z., Komornik, A., & Mazurik, A. (1968). Model study on arching above buried structures. *Journal of the Soil Mechanics and Foundations Division, ASCE, 94*, 1123-1141.

[30]. Finn, W.D.L. (1960). Boundary value problems of soil mechanics. *Journal of the Soil Mechanics and Foundation Division, ASCE, 89*, 39-72.

[31]. Chelapati, C.V. (1964). Arching in soil due to the deflection of a rigid horizontal strip. *Proc, Symposium on Soil-Structure Interaction, University of Arizona, Tucson, Arizona*, pp. 356-377.

[32]. Bjerrum, L., Frimann Clausen, C.J., & Duncan, J.M. (1972). Earth pressures on flexible structures. *Proc, Fifth European Conference on Soil Mechanics and Foundation Engineering, Madrid, Spain*, pp. 169-196.

[33]. Burghignoli, A. (1981). Soil interaction in buried structures. *Proc, Tenth International Conference on Soil Mechanics and Foundation Engineering, Stockholm, Sweden*, pp. 69-74.

[34]. Rui, R., Tol, F., Xia, Y.Y., Eekelen, S., & Hu, H. (2018). Evolution of soil arching: 2D analytical models. *International Journal of Geomechanics, 18(6)*, 04018056.

[35]. Liang, L., Xu, C., Chen, Q., & Chen, Q. (2022). Experimental and theoretical investigations on evolution of soil-arching effect in 2D trapdoor problem. *International Journal of Geomechanics, 20(6)*, 06020007.

[36]. Getzler, Z., Gellert, M., & Eitan, R. (1970). Analysis of arching pressures in ideal elastic soil. *Journal of the Soil Mechanics and Foundations Division, ASCE, 96*, 1357-1372.

[37]. Ranken, R.E., & Ghaboussi, J. (1975). Tunnel design considerations: analysis of stresses and deformations around advancing tunnels. *Department of Transportation, Report No*, FRA-OR and D 75- 84.

[38]. Rude, L.C. (1982). Measured performance of a laboratory culvert. *Journal of the Geotechnical Engineering Division, ASCE, 108*, 1624-1641.

[39]. Stone, K.J.L. (1988). Modeling of rupture development in soils. *PhD dissertation, Wolfson College, Cambridge University*.

[40]. Koutsabeloulis, N.C., & Griffiths, D.V. (1989). Numerical modeling of the trapdoor problem. *Geotechnique, 39*, 77-89.

[41]. Sakaguchi, H., & Ozaki, E. (1992). Analysis of the formation of arches plugging the flow of granular materials. *Proc, the 2nd International Conference on Discrete Element Method, MIT, Cambridge, Massachusetts*, pp. 153-163.

[42]. Bhandari, A. (2010). Micromechanical analysis of geosynthetic–soil interaction under cyclic loading. *PhD dissertation, University of Kansas, Lawrence, KS, USA*.

[43]. George, T.I., & Dasaka, S.M. (2021). Numerical investigation of soil arching in dense sand. *International journal of Geomechanics, 21(5)*, 04021051.

[44]. Su, D., Chen, W., Wang, X., Huang, M., Pang, X., & Chen, X. (2022). Numerical study on transverse deformation characteristics of shield tunnel subject to local soil loosening. *Underground Space, 7*, 106-121.

[45]. Al-Hattamleh, O., Muhunthan, B., & Zbib, H.M. (2022). Soil arching in dry sand: numerical simulations using double-slip plasticity gradient model. *International journal of Geomechanics, 22(2)*.

[46]. Meguid, M.A., Saada, O., Nunes, M.A., & Mattar, J. (2008). Physical modeling of tunnels in soft ground: A review. *Tunnelling and Underground Space Technology, 23*, 185–198.

[47]. Zhao, Y., Gong, Q., Wu, Y., Zornberg, J.G., Tian, Z., & Zhang, X. (2021). Evolution of active arching in granular materials: Insights from load, displacement, strain, and particle flow. *Powder Technology, 384*, 160-175.

[48]. Costa, Y.D., Zornberg, J.G., Bueno, B.S., & Costa, C.L. (2009). Failure mechanisms in sand over a deep active trapdoor. *Journal of Geotechnical and Geo-environmental Engineering, 135(11)*, 1741-1753.

[49]. Iglesia, G.R., Einstein, H.H., & Whitman, R.V. (2011). Validation of centrifuge model scaling for soil systems via trapdoor tests. *Journal of Geotechnical and Geoenvironmental Engineering, 137(11)*.

[50]. Iglesia, R., Einstein, H.H., & Whitman, R.V. (2013). Investigation of soil arching with centrifuge tests. *Journal of Geotechnical and Geo-environmental Engineering, 140(2)*, 04013005.

[51]. Zhang, H., Zhang, P., Zhou, W., Dong, S., & Ma, B. (2016). A new model to predict soil pressure acting on deep burial jacked pipes. *Tunneling and Underground Space Technology, 60*, 183-196.

[52]. Bhandari, A. & Han, J. (2018). Two-dimensional physical modelling of soil displacements above trapdoors. *Geotechnical Research, 5(2)*, 68-80.

[53]. Rui, R., Han, J., Eekelen, S., & Wan, Y. (2019). Experimental investigation of soil-arching development in unreinforced and geosynthetic-reinforced pile-supported embankments. *Journal of Geotechnical and Geoenvironmental Engineering, 145(1)*, 04018103.

[54]. Al-Naddaf, M., Han, J., Xu, C., Jawad, S., & Abdulrasool, G. (2019). Experimental investigation of

soil arching mobilization and degradation under localized surface loading. *Journal of Geotechnical and Geoenvironmental Engineering, 145(2)*, 04019114.

[55]. Ali, U., Otsubo, M., Ebizuka, H., & Kuwano, R. (2020). Particle-scale insight into soil arching under trapdoor condition. *Soils and Foundations, 60*, 1171–1188.

[56]. Moussaei, N., Khosravi, M.H., & Hossaini, M.F. (2022). Physical modeling of soil arching around shallow tunnels in sandy grounds. *International Journal of Mining and Geo-Engineering, IJMGE, 56(4)*, 413-422.

[57]. Zhang, Y., Liu, X., Yuan, S., Song, J., Chen, W., & Dias, D. (2023). A two-dimensional experimental study of active progressive failure of deeply buried Qanat tunnels in sandy ground. *Soils and Foundations*, 63, 101323.

[58]. Khosravi, M. H., Pipatpongsa, T., & Takemura, J. (2013). Experimental analysis of earth pressure against rigid retaining walls under translation mode. *Géotechnique, 63(12)*, 1020-1028.

[59]. Khosravi, M. H., Hamedi Azad, F., Bahaaddini, M., & Pipatpongsa, T. (2017). DEM analysis of backfilled walls subjected to active translation mode. *International Journal of Mining and Geo-Engineering, 51(2)*, 191-197.

[60]. Salehi Alamdari, N., Khosravi, M. H., & Katebi, H. (2020). Distribution of lateral active earth pressure on a rigid retaining wall under various motion modes. *International Journal of Mining and Geo-Engineering, 54(1)*, 15-25.

[61]. Khosravi, M. H., Kargar, A. R., & Amini, M. (2020). Active earth pressures for non-planar to planar slip surfaces considering soil arching. *International Journal of Geotechnical Engineering, 14(7)*, 730-739.

[62]. Khosravi, M.H., Sarfaraz, H., Pipatpongsa, T. & Sharifdeljuyi, A. (2022). Active Earth Pressure Distribution inside Narrow Backfill Considering Soil-Arching Effect. *International Journal of Geomechanics, 22(7)*, 06022013.

[63]. Sarfaraz, H., Khosravi, M.H., & Pipatpongsa, T. (2023). Theoretical and Numerical Analysis of Cohesive-Frictional Backfill against Battered Retaining Wall under Active Translation Mode. *International Journal of Geomechanics, 23(6)*, 04023079.

[64]. Khosravi, M. H., Pipatpongsa, T., Takahashi, A., & Takemura, J. (2011). Arch action over an excavated pit on a stable scarp investigated by physical model tests. *Soils and foundations, 51(4)*, 723-735.

[65]. Khosravi, M., Tang, L., Pipatpongsa, T., Takemura, J., & Doncommul, P. (2012). Performance of counterweight balance on stability of undercut slope evaluated by physical modeling. *International Journal of Geotechnical Engineering, 6(2)*, 193-205.

[66]. Khosravi, M. H., Takemura, J., Pipatpongsa, T., & Amini, M. (2016). In-flight excavation of slopes with potential failure planes. *Journal of Geotechnical and Geoenvironmental Engineering, 142(5)*, 06016001.

[67]. Khosravi, M. H., Sarfaraz, H., Esmailvandi, M., & Pipatpongsa, T. (2017). A numerical analysis on the performance of counterweight balance on the stability of undercut slopes. *International Journal of Mining and Geo-Engineering, 51(1)*, 63-69.

[68]. Khosravi, M. H., Pipatpongsa, T., Takemura, J., & Amini, M. (2017). Influence of modeling material on undercut slope failure mechanism. *Journal of Mining and Environment, 8(4)*, 645-662.

[69]. Ukritchon, B., Ouch, R., Pipatpongsa, T., & Khosravi, M. H. (2018). Investigation of stability and failure mechanism of undercut slopes by three-dimensional finite element analysis. *KSCE Journal of Civil Engineering, 22*, 1730-1741.

[70]. Sarfaraz, H., Khosravi, M. H., Pipatpongsa, T., & Bakhshandeh Amnieh, H. (2021). Application of artificial neural network for stability analysis of undercut slopes. *International Journal of Mining and Geo-Engineering, 55(1)*, 1-6.

[71]. Sarfaraz, H., Khosravi, M. H., & Pipatpongsa, T. (2021). Numerical Stability Analysis of Undercut Slopes Evaluated by Response Surface Methodology. *Journal of Mining and Environment, 12(1)*, 31-43.

[72]. Nasiri, F., Khosravi, M. H., & Takemura, J. (2022). An experimental study of pile stabilized infinite slopes under in-flight pseudo-static loading. *Bulletin of Engineering Geology and the Environment, 81(10)*, 440.

[73]. Sarfaraz, H., Khosravi, M.H., Pipatpongsa, T. & Saedi, G. (2023). Estimation of passive earth pressure against a battered rigid retaining wall in cohesive-frictional backfill, *Journal of Geomine, 1(1)*, 22-29.

[74]. Han, J., Wang, F., Nadfaf, M., & Xu, C. (2017). Progressive Development of Two-Dimensional Soil Arching with Displacement. *International Journal of Geomechanics, 17(12)*.

[75]. Li, L., Dube, J.S., & Aubertin, M. (2013). An extension of Marston's solution for the stresses in backfilled trenches with inclined walls. *Geotechnical and Geological Engineering, 31*, 1027–1039.

[76] Atkinson, J.H., & Potts, D.M. (1977). Stability of a shallow circular tunnel in cohesion less soil. *Géotechnique, 27(2)*, 203.–215.

[77]. Rui, R., Tol, A.F., Xia, Y. Y., Eekelen, S. J. M., & Hu, G. (2016). Investigation of soil-arching development in dense sand by 2D model tests. *Geotechnical Testing Journal, 39(3)*, 20150130.

[78]. Marshall, A.M. (2009). Tunneling in sand and its effect on pipelines and piles. *Thesis, Department of Engineering, University of Cambridge*, 270 p.

[79]. Zhou, B. (2014). Tunneling-induced ground displacements in sand. *PhD thesis, University of Nottingham*, 227 p.

[80]. Franza, A. (2016). Tunneling and its effects on piles and piled structures. *Thesis, Department of Civil Engineering University of Nottingham*, 279 p.

[81]. Khatami, H.R. (2018). A study of arching effect in soils incorporating recycled tyres. *School of Civil, Environmental and Mining Engineering, Faculty of Engineering, Computer and Mathematical Sciences, University of Adelaide*, 255 p.

[82]. Moussaei, N., Khosravi, M.H., & Hossaini, M.F. (2019). Physical modeling of tunnel induced displacement in sandy grounds. *Tunneling and Underground Space Technology, 90*, 19-27.

[83]. Song, G., & Marshall, A.M. (2020). Centrifuge modelling of tunneling induced ground displacements: pressure and displacement control tunnels. *Tunneling and Underground Space Technology, 103*, 103461.

[84]. Janelid, I., & Kvapil, R. (1966). Sublevel caving. *International Journal of Rock Mechanics and Mining Science, 3(2)*, 129-153.

[85]. Wu, J., Liao, S.M., & Liu, M.B. (2019). An analytical solution for the arching effect induced by ground loss of tunneling in sand. *Tunneling and Underground Space Technology, 83*, 175-186.

[86]. Lee, C.J., Chiang, K.H., & Kuo, C.M. (2004). Ground movement and tunnel stability when tunneling in sandy ground. *Journal of the Chinese Institute of Engineers, 27(7)*, 1021-1032.

[87]. Lee, C.J., Chen, P.S., & Chiang, K.H. (2006). Evolution of arching effect during tunneling in sandy soil. *The 4th dimension of metropolises, Taloy and Francis, Hong Kong*, pp. 1171-1176.

[88]. Shahin, H. M., Nakai, T., Zhang, F., Kikumoto, M., Tabata, Y., & Nakahara, E. (2007). Model tests and numerical simulations on shallow circular tunneling. *Proc, the 19th Central Japan Geotechnical Symposium, Nagoya, Japan,* pp. 131–138.

[89]. Long, Y.Y., & Tan, Y. (2020). Soil arching due to leaking of tunnel buried in water-rich sand. *Tunneling and Underground Space Technology, 95*, 103158.

مروری بر پدیده قوس‌زدگی تنش و تغییرشکل محیط اطراف تونل در زمین‌های ماسه‌ای

قربان خاندوزی[۱] و محمد حسین خسروی[۲*]

۱. دانشکده مهندسی معدن، دانشکدگان فنی، دانشگاه تهران، تهران، ایران

۲. گروه مهندسی معدن، دانشکده مهندسی، دانشگاه بیرجند، بیرجند، ایران

ارسال ۲۰۲۳/۰۹/۳۰، پذیرش ۲۰۲۳/۱۱/۱۴

* نویسنده مسئول مکاتبات: mh.khosravi@birjand.ac.ir

چکیده:

آب‌های زیرزمینی یک منبع ضروری برای بقای انسان هستند، اما کیفیت آن اغلب توسط فعالیت‌های انسانی مانند دفع نادرست زباله‌ها کاهش می‌یابد. شیرابه تولید شده از محل‌های دفن زباله می‌تواند آب‌های زیرزمینی را آلوده کند و مشکلات زیست محیطی و بهداشتی شدیدی را ایجاد کند. تکنیک‌های یادگیری ماشینی را می‌توان برای پیش‌بینی کیفیت آب‌های زیرزمینی و ویژگی‌های شیرابه برای مدیریت مؤثر این موضوع مورد استفاده قرار داد. این مطالعه یک مدل مبتنی بر یادگیری ماشینی را برای پیش‌بینی کیفیت آب زیرزمینی و ویژگی‌های شیرابه با استفاده از شاخص کیفیت آب موثر (EWQI) پیشنهاد می‌کند. مجموعه داده شیرابه مورد استفاده در این مطالعه از محل دفن زباله و مجموعه داده‌های کیفیت آب زیرزمینی از بررسی ادبیات جمع آوری شد. میانگین مقادیر TDS، Ca، Mg، NO3- و PO4- از حد تجویز شده برای اهداف آب آشامیدنی فراتر رفت. مدل پیشنهادی از معماری یادگیری ماشین مبتنی بر یک شبکه عصبی کانولوشن (CNN) برای استخراج ویژگی‌های مرتبط از داده‌های ورودی استفاده می‌کند. سپس ویژگی‌های استخراج‌شده به یک شبکه کاملاً متصل برای تخمین EWQI نمونه‌های ورودی وارد می‌شوند. این مدل که بر روی مجموعه داده‌های کیفیت شیرابه و آب زیرزمینی آموزش دیده و آزمایش شده است، به دقت و کارایی محاسباتی بالایی دست می‌یابد و به پیش‌بینی کیفیت آب زیرزمینی و ویژگی‌های شیرابه برای مدیریت پسماند کمک می‌کند.

کلمات کلیدی: همگرایی تونل، قوس‌زدگی، توزیع مجدد تنش، باندهای برشی غیرخطی، ناحیه سست شده اطراف تونل.